Austrian Journal of Technical and Natural Sciences

№ 3–4 2019
March– April

PREMIER
Publishing

Vienna
2019

Austrian Journal of Technical and Natural Sciences

Scientific journal

№ 3–4 2019 (March– April)

ISSN 2310-5607

Proofreading Kristin Theissen

Cover design Andreas Vogel

Additional design Stephan Friedman

Editorial office Premier Publishing s.r.o.
Praha 8 – Karlín, Lyčkovo nám. 508/7, PSČ 18600

E-mail: pub@ppublishing.org

Homepage: ppublishing.org

Austrian Journal of Technical and Natural Sciences is an international, German/English/Russian language, peer-reviewed journal. It is published bi-monthly with circulation of 1000 copies.

The decisive criterion for accepting a manuscript for publication is scientific quality. All research articles published in this journal have undergone a rigorous peer review. Based on initial screening by the editors, each paper is anonymized and reviewed by at least two anonymous referees. Recommending the articles for publishing, the reviewers confirm that in their opinion the submitted article contains important or new scientific results.

Premier Publishing s.r.o. is not responsible for the stylistic content of the article. The responsibility for the stylistic content lies on an author of an article.

Instructions for authors

Full instructions for manuscript preparation and submission can be found through the Premier Publishing s.r.o. home page at:
http://ppublishing.org.

Material disclaimer

The opinions expressed in the conference proceedings do not necessarily reflect those of the Premier Publishing s.r.o., the editor, the editorial board, or the organization to which the authors are affiliated.

Premier Publishing s.r.o. is not responsible for the stylistic content of the article. The responsibility for the stylistic content lies on an author of an article.

Included to the open access repositories:

ULRICHSWEB™ GLOBAL SERIALS DIRECTORY

Typeset in Berling by Ziegler Buchdruckerei, Linz, Austria.
Printed by Premier Publishing s.r.o., Vienna, Austria on acid-free paper.

Section 1. Medical science

Sadirkhodjaeva Azizakhon Alavitdinovna,
Doctoral student of the 1st course of the Ph.D.
of the Department of Pediatric Diseases, Hematology; TashPMI
E-mail: azizanew@mail.ru

Ashurova Dilfuza Tashpulatovna,
Ph.D. associate professor, head of the department
propedeutics of children's diseases, hematology; TashPMI

FEATURES OF THE STATE OF CARDIAC MARKERS IN THE EARLY DIAGNOSIS OF DIABETIC CARDIOMYOPATHY IN CHILDREN WITH TYPE1 DIABETES

Abstract. Type 1 diabetes mellitus (DM1) is an autoimmune disease associated with the destruction of insulin-producing pancreatic β-cells, the genesis of which involves many genetic and immunological factors. When T1DM, antibodies to β-cells are present. It has been shown that in 1/3 of the cases the autoimmune process is not limited to betta cell lesions and other autoimmune diseases develop.

Keywords: diabetes mellitus, CF creatinine phosphakinase, highly sensitive CRP.

Садирходжаева Азизахон Алавитдиновна,
Докторант 1 курса Ph.D. кафедры пропедевтики
детских болезней, гематологии; ТашПМИ
E-mail: azizanew@mail.ru

Ашурова Дилфуза Ташпулатовна,
Д.м.н., доцент, заведющая кафедры
пропедевтики детских болезней, гематологии; ТашПМИ

ОСОБЕННОСТИ СОСТОЯНИЯ КАРДИОЛОГИЧЕСКИХ МАРКЁРОВ В РАННЕЙ ДИАГНОСТИКИ ДИАБЕТИЧЕСКОЙ КАРДИОМИОПАТИИ У ДЕТЕЙ С САХАРНЫМ ДИАБЕТОМ 1 ТИПА

Аннотация. Сахарный диабет 1-го типа (СД1) представляет собой аутоиммунное заболевание, связанное с деструкцией инсулинпродуцирующих β-клеток поджелудочной железы, в генез которого вовлечены многие генетические и иммунологические факторы. При СД1 присутствуют антитела к β-клеткам. Показано что в 1/3 случаев аутоиммунный процесс не ограничивается поражением бетта клеток и развиваются другие аутоиммунные заболевания.

Ключевые слова: сахарный диабет, МВ креатининфосфакиназа, высокочувствительный СРБ.

Актуальность. Поздние осложнения сахарного диабета I типа, в том числе и со стороны сердечно-сосудистой системы, являются основной причинойраннейинвалидизацииивысокойлетальности больных, что определяет медицинскую и социальную значимость данного заболевания [1; 2]. Прогрессирование сахарного диабета приводит к развитию кардиомиопатии, миокардиосклероза сердечной недостаточности, жизнеугрожающих нарушений сердечного ритма и внезапной сердечной смерти [3; 4].

В основе развития диабетической кардиомиопатии лежат три патогенетических механизма: 1) метаболические нарушения (гипергликемия, повышенная утилизация свободных жирных кислот, гипоксия тканей, электролитные нарушения); 2) диабетическая микроангиопатия и; 3) автономная кардиоваскулярная нейропатия [5; 6]. Они приводят к энергетическому дефициту миокардиоцитов и клеток проводящей системы сердца, что в свою очередь способствует развитию ультраструктурных и функциональных изменений в миокарде [7].

Цель исследования: установить критерии ранней диагностики диабетической кардиомиопатии, для разработки алгоритма диагностики, лечения и профилактики ее прогрессирования и установить частоту встречаемости сопутствующих заболеваний с данной патологией.

Материал и методы. Обследованы 46 детей в возрасте от 8 до 17 лет с сахарным диабетом длительностью от нескольких месяцев до 15 лет. Средний возраст детей составил 13,3 года. На период обследования ни у кого из больных не отмечалось кетоацидотических и гипогликемических состояний. Все дети были разделены на 2 группы в зависимости от длительности заболевания 1-ю группу составил 20 детей с длительностью сахарного диабета до 5 лет, 2-ю группу – 26 детей с длительностью заболевания более 5 лет.

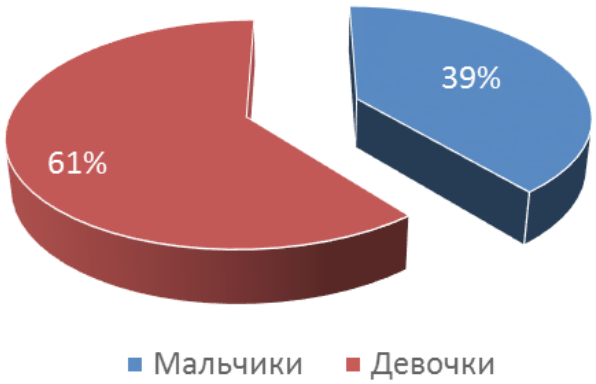

Рисунок 1. Распределения больных по полу

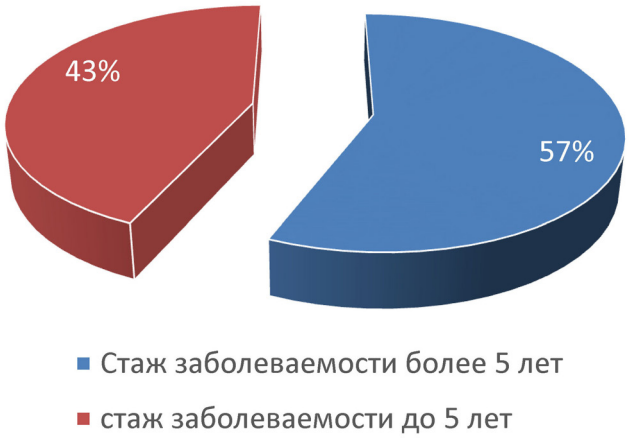

Рисунок 2. Распределения детей по стажу заболеваемости

Результаты. В основе развития поздних осложнений сахарного диабета у детей, в том числе со стороны сердечно-сосудистой системы, лежат метаболические нарушения, связанные с неудовлетворительной компенсацией заболевания, которая, по нашим данным, выходит из под контроля при длительности сахарного диабета более 5 лет. Это подтверждается тесной прямой корреляционной связью уровня HbA1c с длительностью болезни.

При сопоставлении данных стажа заболевания и гликированного гемоглобина било установлено прямая достоверная взаимосвязь, т.е. с увеличением стажа, гликированный гемоглобин повышается.

Учитывая вышеуказанные данные длительность болезни и уровень HbA1c, как показателя метабо-

лического дисбаланса достаточно надежно коррелирует с органными и системными осложнениями. Можно предположит, что ведущее значение в развитии органной патологии имеют не максимальные пики подъёма концентрации глюкозы в крови, а длительно сохраняющаяся гипергликемия.

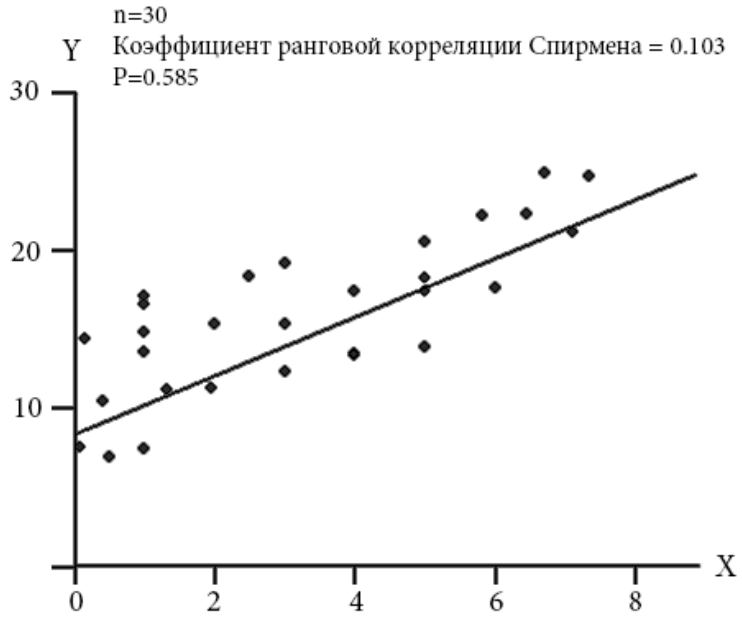

Рисунок 3. Корреляционная связь между стажем заболевания и гликированным Hb

Примечания: ось X – значения стажа; Y – значения гликированного гемоглобина

Следовательно, у детей с длительностью сахарного диабета более 5 лет возрастает риск развития поздних осложнений заболевания, что требует пристального внимания врачей с целью их раннего выявления и своевременной профилактики дальнейшего.

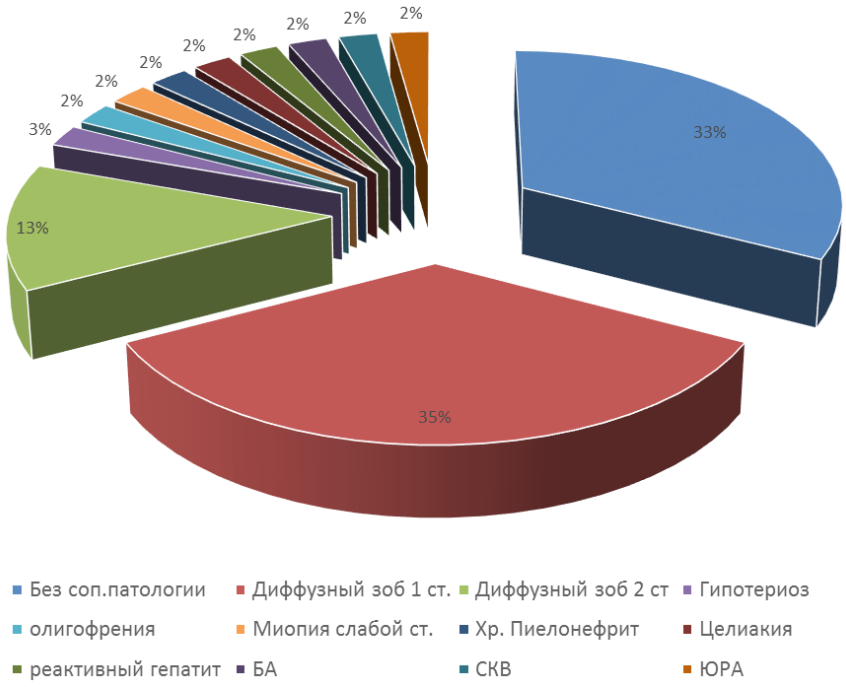

Рисунок 4. Сопутствующая патология больных с сахарным диабетом 1 типа

Сахарный диабет 1-го типа представляет собой аутоиммунное заболевание, связанное с деструкцией инсулинпродуцирующих β-клеток поджелудочной железы, в генез которого вовлечены многие генетические и иммунологические факторы. При СД1 присутствуют антитела к β-клеткам и имеет место инсульт.

По результатом исследования можно увидит что СД 1 типа чаше встречается вместе с диффузным зобом (48%), а с другими аутоиммунными патологиями такие как: целиакия, бронхиальная астма, системная красная волчанка, ювенильный ревматоидный артрит, реактивный гепатит встречался в одинаковых количествах (2%).

В результате исследования установлено, что у большинства детей с сахарным диабетом определяется повышения в биохимическом анализе крови показателя кардиологического маркёра. в том числе МВ-КФК и высокочувствительной фракции СРБ. В первой группе показатель МВ-КФК составило в среднем 28мг/л, во второй группе 32 мг/л. и повышения высокочувствительной фракции СРБ в основном определялось у детей со стажем заболевания более 5 лет (5,2мг/л)

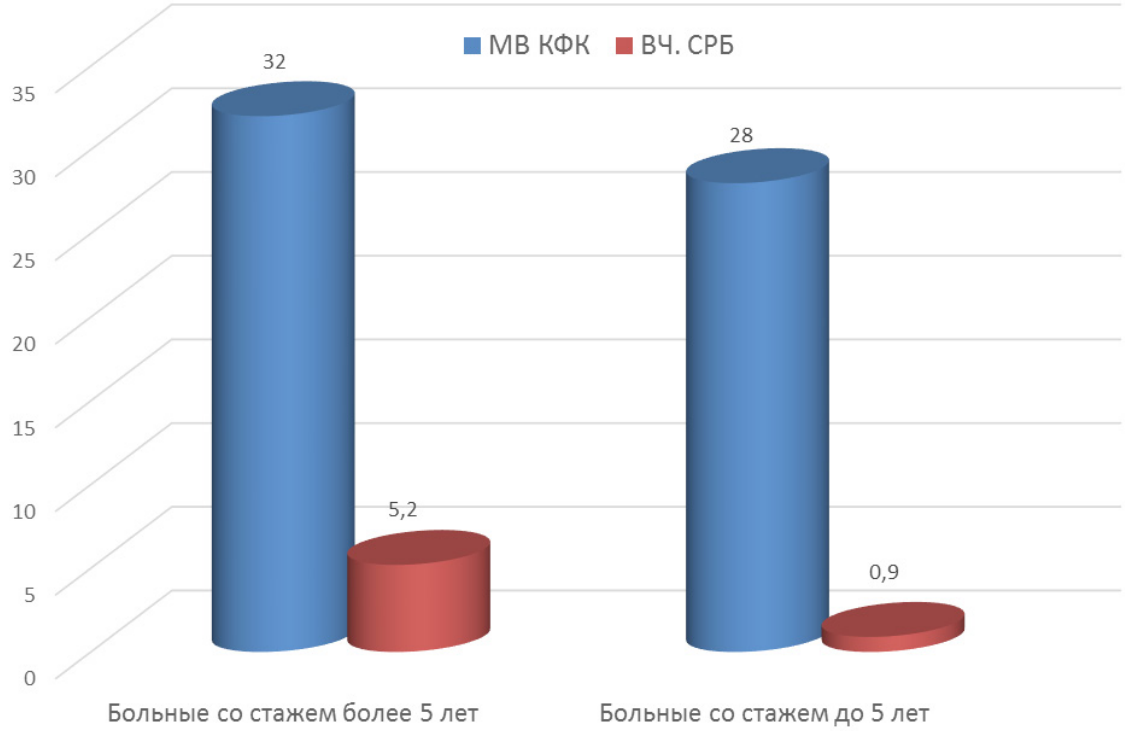

Рисунок 5. Показатели кардиального маркёра в зависимости от стажа заболеваемости

Выводы 1. У пациентов с СД1 повышен риск других аутоиммунных заболеваний. Раннее выявление АТ-маркеров аутоиммунных заболеваний и скрытых нарушений функции органов-мишеней позволят предотвратить развитие тяжёлой и в некоторых случаях жизнеугрожающей клинической манифестации заболевания, способной ухудшать течение СД1.

2. Таким образом, установленные нами критерии ранней диагностики диабетической кардиомиопатии у детей и роль повышения показателя МВ КФК и высокочувствительной фракции СРБ позволяют рекомендовать для практического применения алгоритм диспансерного наблюдения за детьми с сахарным диабетом.

Список литературы:

1. Алимова И. Л. Формирование сердечно-сосудистых осложнений при сахарном диабете I типа у детей и их коррекция. Автореф. дис. … докт. мед. наук. – Смоленск, 2004. – 46 с.
2. Шестакова М. В., Ярек-Мартынова И. Р., Кухаренко С. С. и др. Кардиоренальная патология при сахарном диабете типа 1: механизмы развития и возможности медикаментозной коррекции. Тер архив 2005; 6: 40–45.
3. Гречкин В. И., Ромашов Б. Б., Ряскина В. В., Нечепоренко Л. Н. Нарушение диастолической функции левого желудочка как причина сердечной недостаточности у больных сахарным диабетом. Кардиология, основанная на доказательствах. – М., 2000. – 79 с.
4. Школьникова М. А. Жизнеугрожающие аритмии у детей. – М., 1999. – 230 с.
5. Plante G. E., Chakir M., Ettaouil K. et al. Consequences of alteration in capillary permeability. Can J Physiol Pharmacol 1996; 74: 7: 824–833.
6. Arslan N., Azal O., Kizilmaz A. et al. Assesment of left ventricular diastolic function with Doppler echocardiography in Type-1 Diabetic patients. Diabetologia 1994; 37: 1: 186.
7. Левина Л. И. Сердце при эндокринных заболеваниях. – Л., 1989. – 263 с.

Saidova Nilufar Akhrorovna,
Bukhara State Medical Institute
E-mail: sai-nilufar@mail.ru

COMPLEX TREATMENT OF ADOLESCENT (JUVENILE) HYPERTROPHIC GINGIVITIS WITH THE HELP OF VECTOR APPARATUS IN UZBEKISTAN

Abstract. The article is devoted to the actual problem of the effectiveness of complex treatment of young patients with hypertrophic gingivitis in Uzbekistan using the Vector apparatus with the inclusion of microcirculation indicators to evaluate the effectiveness criteria of the complex treatment being carried out.

Keywords: Vector apparatus, juvenile hypertrophic gingivitis, vector therapy.

Introduction. In the adolescent period, marked changes occur in the activity of various endocrine glands. Strengthening the function of the sex glands during puberty has a significant impact on the activity of other endocrine glands and can disrupt the hormonal balance that a child had during childhood. Full activity of the endocrine system ensures the normal course of metabolic processes in the body. Disruption of hormone production causes a breakdown of metabolic processes and the function of tissues and organs. This is reflected in the oral mucosa, regardless of excessive or insufficient function of the endocrine glands.

According to studies, in Uzbekistan, 40% of children in adolescence have gingivitis, while 7% have hypertrophic. Gingival lesions that develop in adolescents with characteristic localization in the area of the anterior teeth are called juvenile gingivitis.

a) b)

Figure 1.

Juvenile gingivitis may occur in girls 1/2–1 years before their menstruation. There is a dependence of the development of inflammatory changes in the gums with menstruation: the activation of the inflammatory process in the gums before each menstruation occurs in 2–3 days, its decline is noted on the 2–5th day of menstruation. Often, hormonal gingivitis is accompanied by an increase in tooth mobility due to osteoporosis of the jaw bone tissue.

In our country, the effectiveness of treatment of juvenile hypertrophic gingivitis remains an urgent task, despite the large selection of anti-inflammatory drugs. It is necessary to take into account the pathophysiological changes in the body of adolescents that occur in tissues with periodontal diseases and the possibility of exposure to pathogenesis links. Thus, with the combined effect of ultrasonic vibrations, hydrodynamic effects and the use of hydroxylapatite, the biofilm

containing bacteria is easily removed, and the inflammatory processes in the periodontium subsequently disappear. Clinical and experimental studies revealed a high efficiency of the combination of low-intensity ultrasonic vibrations. Moreover, hydroxylapatite is a mineral substance that is biocompatible with the human body, which is part of the tooth enamel and is used in the treatment of periodontal disease.

When using vector technology: there is no mechanical damage to the tooth and root due to gentle and atraumatic removal of biofilm. The doctor does not scrub the surface of the root, but produces tool movements from the outside to the bottom of the pocket, working along the root; the patient does not feel pain during the procedure. With mechanical manual curettage, in response to an irritant, the body activates a protective immune response. Therefore, the process is complicated by the presence of bleeding, the appearance of supragingival dental deposits, pathological traumatic occlusion and open dentinal tubules. Complications such as gingival recession and lysis of bone structures are possible. Due to the scraping: a glassy surface is formed; possible damage to the cement root; there is a violation of all structures that are important for regeneration. Thanks to the suspension, which contains hydroxyapatite microparticles, the efficiency of cleaning the root of the tooth significantly increases, and the periodontal pocket is intensively processed and washed.

Purpose of the study. To increase the effectiveness of the treatment of chronic juvenile hypertrophic gingivitis, speed up the treatment time.

Objectives of the study.

1. To prove the high effectiveness of the complex therapy of gingivitis using the combined method of treatment of ultrasound exposure and the use of hydroxyapatite.

2. To determine the change in the degree of edema in patients with chronic hypertrophic gingivitis and its exacerbation.

Materials and methods.

The main group of patients was 40 patients with hypertrophic gingivitis aged 13–16 years (20 with a chronic course and 20 with an exacerbation of chronic gingivitis). All patients underwent a comprehensive examination of the dental status.

Comprehensive treatment of patients with inflammatory periodontal diseases included etiological, pathogenetic and symptomatic therapy. As a component of pathogenetic therapy, a combined physiotherapeutic effect of ultrasonic cleaning and hydroxyapatite using the Vector apparatus was used. Ultrasound therapy was performed with the "VECTOR" device using a special nozzle with an optimal shape.

The results of the study. In patients with chronic hypertrophic gingivitis after treatment, there is almost complete recovery of normalized tissue. During exacerbation of chronic hypertrophic gingivitis, the degree of hypertrophy before treatment was 60%, after treatment it decreased to 49.7%. The treatment with combined effects of ultrasound and hydroxylapatite in patients with hypertrophic gingivitis showed a positive clinical effect after 3 sessions, which resulted in a reduction in the size of the papillae, cessation of bleeding of the gums when brushing teeth, and no unpleasant smell from the mouth.

Figure 2. Gingivitis before treatment

Figure 3. Gingivitis after treatment

Discussion. Consequently, the combined treatment carried out using physiotherapeutic methods and hydroxylapatitis restores the violation of the intravascular microcirculation component in young patients with chronic hypertrophic gingivitis.

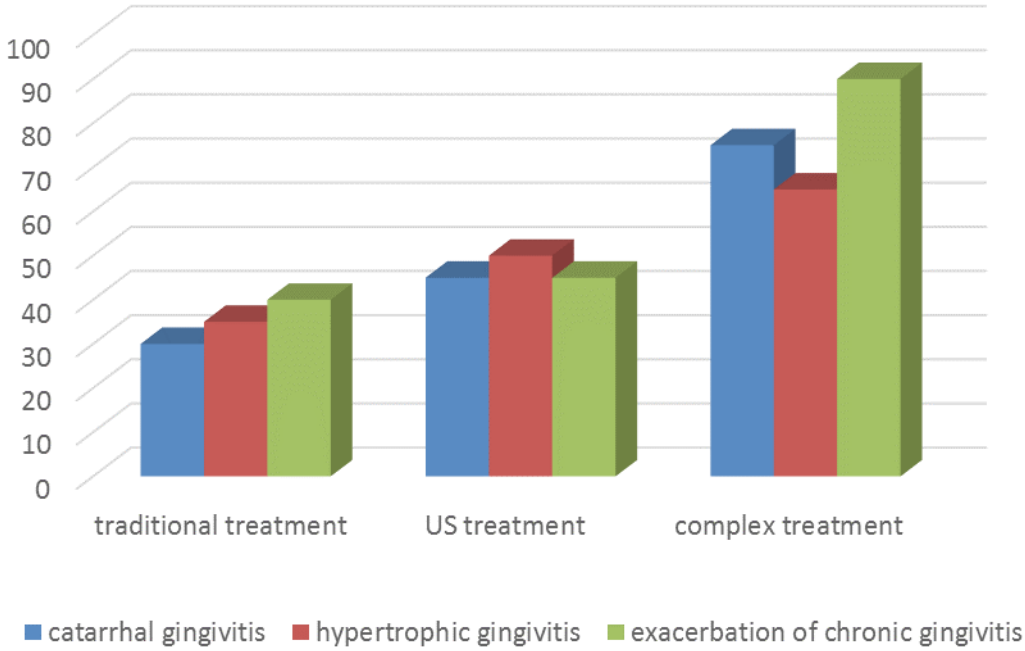

Diagram 1. Of the effectiveness of laser treatment for various forms of gingivitis

Conclusion. Thus, the effectiveness of treatment in patients with juvenile hypertrophic gingivitis is achieved in a shorter time compared with the traditional regimen for the treatment of inflammatory periodontal diseases.

References:

1. Kitaeva V. N., Bulkina N. V., Polosukhina E. N., Parfenova S. V., Kobzeva Yu. A. Research of disturbances of functional activity of thrombocytes in patients with chronic generalized periodontitis with the purpose of early diagnosis of periodontal pathology // Saratov Journal of Medical Scientific Research. 2011. – T. 7. – No. 1 (annex). – P. 295–297.
2. Moskvin S. V., Amirkhanyan A. N. Methods of combined and combined laser therapy in dentistry.– M.– Tver: OOO "Publishing house". Triada ", 2011.– P. 108–109, – P. 121–129.
3. Ivanov P. V., Zudina I. V., Bulkina N. V., Vedyaeva A. P., Ivanova E. V. Anti-inflammatory effect of chitosan ascorbate in the complex therapy of periodontal diseases. Modern problems of science and education. 2013. – No. 4. – 105 p.
4. Bulkina N. V., Borodulin V. B., Osipova Yu. L., Kropotina A. Yu., Guseva O. Yu., Bashkova L. V. Biochemical changes in the saliva of patients with chronic generalized periodontitis under the influence of combined action running alternating magnetic field and laser radiation. Saratov Journal of Medical Scientific Research, 2009. – Vol. 5. – No. 3. – P. 390–393.
5. Kitaeva V. N. Disturbance of aggregation and activity of platelets in patients with periodontal disease: Abstract. honey. Sciences / V. N. Kitaeva.– Saratov, 2007.– 71 p.

Section 2. Food processing industry

Akhmedov Azimjon Normuminovich,
c.t.s., ass.prof. Head of the department "Chemistry" (KEEI)
E-mail: a.ahmedov80@mail.ru; azim-10–86@mail.ru

INCREASING THE TECHNOLOGY OF LIGHTLY REFINED OIL OBTAINED FROM LOW-GRADE COTTON SEEDS

Abstract. This article introduces the technology of initial whitening of low-grade cotton seeds. As a result of the initial injection of urea-modified soil-based adsorbents (MSBA), the amount of cotton oil, acid content and sediment lubricant decreased.

Keywords: gossypol, modified carbamide clay adsorbent, flock but standard newly buttermilk chitlada olingan my, carbamide, pre-lightening.

Introduction

Regarding to the number, a significant amount of low-grade cotton seeds is supplied to the enterprises of the oil and fat industry of the country, processing of which is accompanied by large losses of oil and reagents.

The technology used to produce cottonseed oil is used to process the first and second varieties of cotton seeds and allows to obtain oil and cakes that meet the requirements of the relevant standards [1].

Analysis of crude oils derived from low-grade cotton seeds shows that they contain a significant amount of coloring matter (gossypol, chlorophyll and their derivatives), free fatty acids and other components [2]. Therefore, the selection of a more effective adsorbent for the clarification of these oils is an important scientific and practical task.

Our laboratory studies on the preliminary clarification of these oils showed that it is advisable to use ICHA for this purpose [3].

Cotton oils obtained by pressing and extraction methods from low-grade and non-standard seeds, in most cases, are of dark color and are practically not visible on the Lovibond color meter. This is due to the high content of gossypol, chlorophyll and their derivatives, as well as non-fatty substances.

The existing technology of refining cotton oils obtained from low-grade seeds involves the use of alkaline solutions with a high concentration (400 g /l or more) in an excess amount (150% or more), which leads to significant losses of oil in soap stock and a decrease in the yield of the resulting product.

Improving the technology of obtaining refined pressing and extraction oils from low-grade and non-standard cotton seeds using the method of pre-clarification of raw (black) oils with the help of carbamide-modified clay adsorbent is considered an urgent and practically important task.

At present, domestic and foreign scientists have carried out and are conducting research on the extraction of related substances (including gossypol and its derivatives) from the composition of raw cotton oils obtained by pressing and extraction methods. In the works of A. S. Sadykov, A. L. Markman, V. P. Rzhekhin, A. G. Sergeev, A. I. Glushchenkova, A. I. Ismailov, A. T. Ilyasov and many others. refining cotton oils with solutions of caustic soda,

carbamide and other alkaline reagents. In these methods, due to the high consumption of alkaline reagents, a significant portion of triglycerides is saponified, which adversely affects the yield of the resulting oil and its quality.

Research objective: Development of technology for pre-clarification of raw oils obtained from low-grade and non-standard cotton seeds using a carbamide-modified clay adsorbent.

Objects and research methods: The carbamide-modified clay adsorbents were obtained by impregnating them with a 30% urea solution, followed by drying at 95–1000 °C to a moisture content of 7–8%, and they were used for the preliminary clarification of raw cotton oils. We have proposed the choice of the location of the input MSBA in the technological scheme of preliminary cleaning of raw press oils.

A technological scheme was created at JSC "Koson Oil-Extraction" for clarifying raw cotton oil with a clay adsorbent modified with urea. A distinctive feature of this scheme from the well-known is that at the beginning of the supply line of raw oils in the collection – a fuse tank (bush), a hopper is installed, from which the MCA is supplied to the crude oil, in the required amount, depending on the color of the original oil.

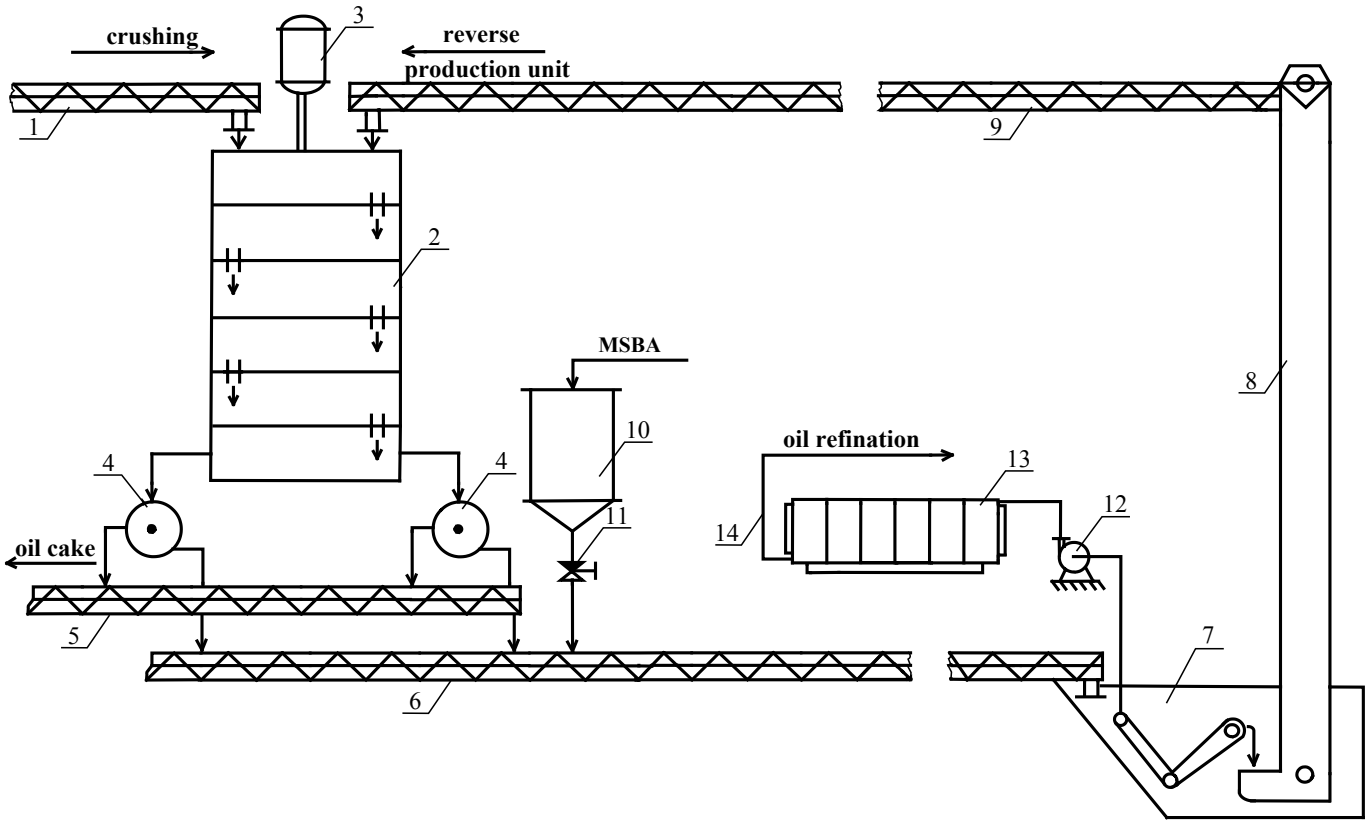

Figure 1. Technological scheme of pre-clarification of raw cotton oil with carbamide-modified clay adsorbent: 1 – steam worm screw; 2 – brazier; 3 – stirrer; 4 – press granulators; 5, 6, 9 and 14 – screw; 7 – fuse tank; 8 – noria; 10 – bunker; 11 – valve; 12 – pump; 13 – filter press

Figure 1 presents the proposed technological scheme for clarification of crude oils, using ICGA. This scheme functions as follows: on auger 1 moistened cotton mint enters the roaster 2, which is equipped with an engine and an agitator 3. From where the pulp enters the press granulators 4, then through the auger 5 the cake is sent to the extraction plant. For the preliminary clarification of crude oils, from the hopper 10 through the valve 11 to the collecting auger of crude oil 6, the loam adsorbent from

Angre kaolin (MCA-4), modified with carbamide, is fed to the batcher in an amount of 2–6% by weight of oil. Further, crude press oil is fed through screw 6 into the fuse tank 7, where it is cleaned of mechanical impurities and sludge. From the fuzo tank 7, the return product (fuz) according to noria 8 and the screw 9 is sent to the roaster 2, and oil is pumped into the frame filter press 13 for filtration, from which they are sent to alkaline refining, and the sediment from the filter press 13 goes to fuza-tank 7.B (табл. 1) представлены технологический режим предварительного осветления сырых масел.

Table 1. – Нормы технологического процесса предварительного осветления сырого масла с использованием МКГА

Name of processes and operations	Unit.	Meanings
I. Moisture Thermal Cotton Mint Treatment:		
– minting of the myatka	%	15–17
– humidity of the mint	%	7–9
– quantity of the return goods (fuse)	%	5–7
II. Pressing and pelletizing:		
– the temperature of the pulp		
– pulp moisture	^{0}C	95–100
– dimensions of grates:	%	7.5–9.5
– first	mm	1.0
– the second	mm	0.75
– the third	mm	0.45
– fourth	mm	0.35
– the size of the matrix for granulation	mm	10–12
III. Preliminary clarification of crude oils:		
– oil temperature	^{0}C	80–90
– number of MKGA	%	5
– time	Per hour	0.4–0.6
IV. Fuza separation:		
– oil temperature	^{0}C	55–70
– speed of turns of a fuse tank	/min	50–60
V. Oil Filtration:		
– oil temperature	^{0}C	70–75
– press pressure	MPa	0.03–0.05

Probably, carbamide with gossiphosphatides according to the substitution principle has the following interaction formula (1):

In addition, urea can form compounds with free fatty acids, their sodium or potassium salts, as well as Schiff bases. Such a complex mechanism of interaction of urea with other components of raw cottonseed oil in the complex is reflected in its color.

Results and their discussion: From the data of Table 1 it can be seen that, in contrast to the traditional technology for producing cottonseed oil, the proposed process introduces the process of clarifying crude oils using an MCA. At the same time, the adjustable parameters of the process of preliminary clarification of raw oils can be the amount of injected ICA and the time of preliminary clarification, which vary in the proposed technological scheme (Fig. 1).

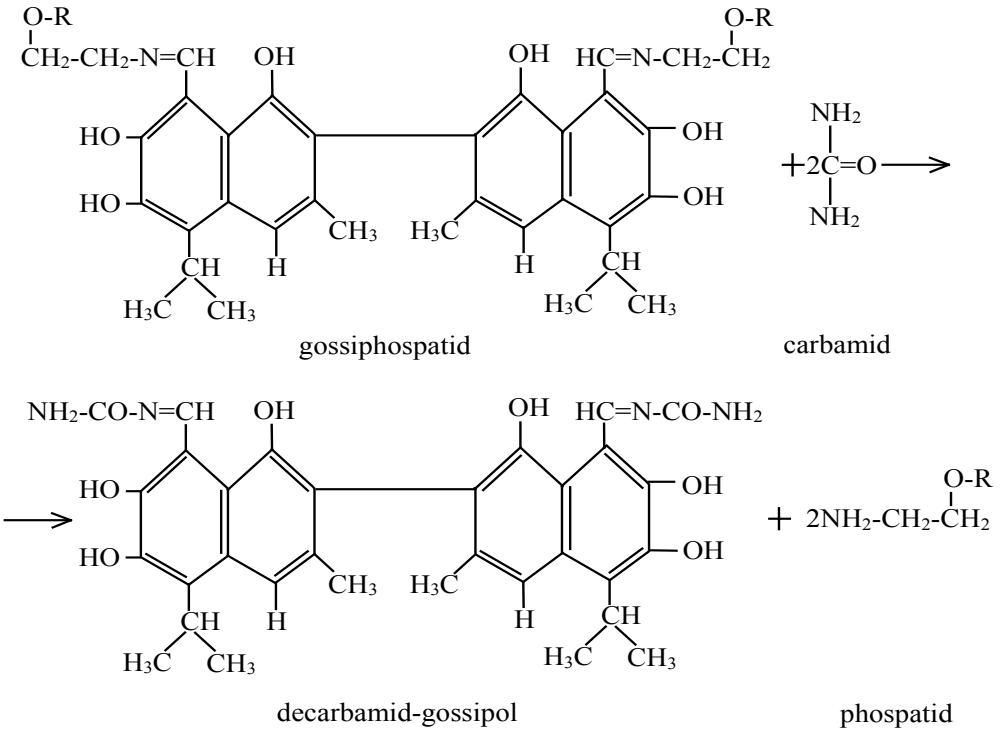

(1)

It is known that the intensive dark color of cottonseed oil is given by the products of changes in native gossypol, as well as melanoidin compounds, which are formed during the self-heating of seeds and heat treatment of mints. In addition, in the process of moisture-heat treatment of cotton myatka, complex compounds of derivatives not only of gossypol, but also of chlorophyll are formed, which also increase the color of the resulting crude oils.

The formation of carbamide compounds with native gossypol is apparently due to the participation of aldehyde groups of the latter, although other mechanisms of their interaction are possible.

In addition, urea can form compounds with free fatty acids, their sodium salts, etc. This complex mechanism of interaction of urea with the accompanying components of raw cottonseed oil in the complex is reflected in its color and other indicators.

In [4], it was shown that the optimal amount of carbide-modified clay adsorbent MKHA-4 when bleaching crude oil obtained from low-grade cotton seeds is 5% by weight.

Table 2. – Indicators of cotton oils, purified in the usual way and pre-clarified using ICGA-4 in the amount of 5% of the total mass of raw materials

Name of cotton oil indicators	**Oil derived from:**	
	low grade seed	**mixtures of low-grade and non-standard seeds**
1	***2***	***3***
Crude oil, purified in the usual way (control):		
Chroma, in 1 cm layer with 70 yellow units:		
– red edinet	65.5	74.3
– siny unity	3.7	6.5
Acid number, mg KOH / g	5.3	6.1
Sludge content,%	0.94	1.85

1	*2*	*3*
Oil, pre-clarified using ICA:		
Chroma, in 1 cm layer with 70 yellow units:		
– red edinet	36.7	42.4
– siny unity	1.5	2.8
Acid number, mg KOH/g	3.2	4.0
Sludge content,%	0.73	0.98

Table 2 presents the results of pre-clarification of crude oils using thermally activated modified adsorbents, for example ICA-4.

From (table 2) it can be seen that the preliminary clarification of crude oils, using 5% of the mass of oil MKGA-4, significantly reduced the color of the oils, their acid numbers and the content of sludge in them. This is explained by the fact that the carbamide-modified clay adsorbent absorbs substances that stain cotton oil and removes them when separating and filtering the oil.

It is known that at present carbamide is used in animal husbandry to enrich feed with non-protein nitrogen. Bentonites and kaolins are also used in the preparation of mixed feed for various purposes. Therefore, the choice of urea and natural clays in obtaining a modified adsorbent becomes reasonable.

Conclusions: Thus, the use of carbamide-modified clay adsorbent MKHA-4 in the process of preliminary clarification of raw oils obtained from low-grade cotton seeds has significantly reduced their color, sludge content and acid number.

References:

1. Kopeykovsky V. M., Danilchuk S. I., Garbuzova G. I. and others. The production technology of vegetable oils.– M .: Light and food industry, 1982. – 416 p.
2. Akhmedov A. N., Abdirakhimov A. S., Dustmurodova S. Zh. Physico-chemical indicators of the prepeso oil obtained from low-grade cotton seeds // "Chemistry and chemical technologist".–Tashkent, 2018. – No. 1. – P. 75–78.
3. Akhmedov A. N., Suvanova F. U., Abdurakhimov S. A., Ikromov O. A. Investigation of the process of refining oils obtained from low-grade cotton seeds // "Chemistry and chemical technologist".– Tashkent, 2014. – No. 3. – P. 69–72.
4. Akhmedov A. N. Improving the technology of complex refining of oils obtained from low-grade cotton seeds. Dissertation of c.t.s.– Karshi, 2012. – 110 p.

Ismatov S. Sh.
Bukhara engineering-technology institute
Associate Professor Mamatkulov Farrukh Golibzhonovich
the teacher of Karshi engineering-economics institute.
E-mail: azim-10–86@mail.ru

RESEARCH OF CHANGES IN THE QUALITY INDICATORS OF BLEACHED COTTONSEED OIL AND ITS PRODUCTS

Abstract. The optimal technological regimes for the partial neutralization of raw cottonseed oil were determined, ensuring the maximum elimination of phospholipids, gossypol and its derivatives, tocopherols from the raw material at the preliminary refining stage. Technique and technology of refining fats continuously improved. On the basis of the work of scientists and the experience of the foremost workers, original technological schemes have been created that ensure a high oil purification effect with a significant reduction in waste and losses. Refining production is equipped with modern high-performance equipment of continuous action, due to which the capacity of workshops is increased and labor costs are significantly reduced.

Key words: phospholipids, gossypol, cotton fat, alkaline refining.

The refinement of vegetable oils and fats is one of the most important technological processes of fat processing. The technology of refining, namely, alkaline neutralization of raw cottonseed oil consists of a complex of complex physical, chemical and physicochemical processes, on which the physic-chemical characteristics and quality indicators of refined oil mainly depend. Technological regimes, yield and quality indicators of refined cottonseed oil are also due to the nature and method of production of raw oil, the composition and the quantitative content of impurities in it, as well as related substances. Selection of an effective adsorbent for the improvement of cotton fat requires a deep study of its mineral and chemical composition, as well as structural properties. The optimal technological regimes for the partial neutralization of raw cottonseed oil were determined, ensuring the maximum elimination of phospholipids, gossypol and its derivatives, tocopherols from the raw material at the preliminary refining stage. Technique and technology of refining fats continuously improved. On the basis of the work of scientists and the experience of the foremost workers, original technological schemes have been created that ensure a high effect of refining oils with a significant reduction in waste and losses. Refining production is equipped with modern high-performance equipment of continuous action, due to which the capacity of workshops increases and labor costs are significantly reduced [1].

The issue of the development and research of the technology of refining oils and fats, as well as the study of the scientific and theoretical foundations of this process, both in the domestic and foreign literature and patent information, is a lot of work. Given this, the issues that are directly related to the topic of my work are analyzed.

For alkaline neutralization of raw cottonseed oil, sodium hydroxide solutions with various concentrations and excess are mainly used as alkaline agents. Refining of raw pre-press and extraction cottonseed oil proceeds at high concentrations and an excess of alkaline sodium hydroxide solution. This technology of refining is accompanied by a low yield of the final product, as well as a significant consumption of material and technological resources. Along with

this, the oil and fat industry of the republic is experiencing a deficiency of sodium hydroxide due to its high cost. Taking this into account, in recent times, advanced technological processes of alkaline neutralization of raw cotton oil have been proposed using new types of alkali-replacing chemical reagents. In this direction, a special place belongs to the use of alkaline-berybamide and other solutions. However, the technological processes of purification of raw cotton oil with these types of alkaline reagents are also not without some drawbacks [1].

It should be noted that the chemical and oil refining industries of the republic use various alkaline solutions in technological processes. At the same time, alkaline compounds of various metals accumulate as industrial wastes and in wastewater. This is especially noticeable with the activation of stationary catalysts used in technological processes of oil refining, cracking and catalytic hydrogenation of oils and fats. Alkaline activation of alloyed stationary aluminum-containing catalysts is carried out using sodium hydroxide solutions. As a result of catalyst activation, alkaline solutions of sodium aluminates are formed, which later, being industrial waste, are discharged into wastewater [2]. However, alkaline solutions of sodium aluminate have a high neutralizing and adsorption capacity. This is especially important when neutralizing the free fatty acids of raw cotton oils. At the same time, alkaline solutions of sodium aluminate react with the substances associated with cottonseed oil. In addition, aluminum compounds and aluminosilicates have high adsorption properties, which is important when combining methods of neutralization and adsorption purification of raw materials. All this determines the prospects and effective use of alkali-containing industrial waste, in particular, sodium aluminate solutions in the oil and fat industry of the republic, namely, in technologies for alkaline neutralization of raw cotton oil. Considering the above, the main objectives of the research on the subject of this thesis were established:

– study of technological processes of alkaline neutralization of raw cotton oil with sodium aluminate solutions of different concentrations and excess;

– determination of the possibility and effectiveness of the use of alkaline solutions of sodium aluminate in the industrial technology of cotton oil refining;

– development of technological regimes and conditions for improving the quality and nutritional value of refined cottonseed oil.

In studies on the alkaline neutralization of raw materials with solutions of aluminates and sodium hydroxide, cotton oil samples were used, obtained by forpressing and extracting oil seeds of cotton of different quality.

The feedstock differed in quality indicators and physico-chemical characteristics [4].

Crude cottonseed oil obtained by forpressing cotton pulp of various varieties of cotton seeds under production conditions was estimated by acid number, color, humidity, content of phospholipids, gossypol and its derivatives. The physic-chemical characteristics of pre-press cotton oils are given in (table 1).

Table 1. – Physic-chemical characteristics of samples of prepress cotton oils

Sample, №	Cotton seed grade	Crudeoilperformance						
		Acid number, mg KOH / g	Humidity,%	Chromaticity, kr.ed. at 35 went. in 1 cm.sl.	Content in %			
					Phospholipids	Free gossypol	Bound Gossypol	General tocopherolcontent, mg 100
1	*2*	*3*	*4*	*5*	*6*	*7*	*8*	*9*
1.	I	3.5–4.7	0.20–0.21	17–21	0.3–0.4	0.09–0.17	0.12–0.20	90–100

1	*2*	*3*	*4*	*5*	*6*	*7*	*8*	*9*
2.	I–II	4.8–6.3	0.22–0.24	23–34	0.5–0.7	0.19–0.23	0.26–0.29	80–90
3.	III – IV	6.9–10.8	0.25–0.27	not super-vised	0.8–1.4	0.29–0.35	0.34–0.39	75–85
4.	Nonstandard	12.2–14.0	0.28–0.31	not super-vised	1.3–1.7	0.44–0.50	0.50–0.65	60–70

As shown by the data given in(table 1). The used samples of pre-press cotton oils differ among themselves by their quality and physic-chemical parameters. At the same time, in raw cottonseed oil obtained from low-grade and non-standard oil seeds, there is an increase in color, the content of free fatty acids and bound gossypol, as well as a decrease in the total amount of tocopherols. In order to obtain extraction oil, the cake of the above samples (Table 1.) Cotton seeds were extracted under production conditions. Physic-chemical characteristics of the obtained extraction of cotton oils are given in (table 2).

It has been established that, in contrast to raw prepressions, extraction oils are characterized by a higher content of free fatty acids, free and bound gossypol, and also phospholopids.

The purpose of this section is to study the effect of the concentration of alkaline solutions on the change in the content of the main accompanying substances of raw cotton oil with the processing of solutions in the electromagnetic field and without it.

Table 2. – Physical and chemical indicators of samples of extraction cotton oils

Sample, № (On the table 2)	**Crudeoilperformance**							
	Acid number, mg KOH / g	**Humidity,%**	**Chromaticity, kr.ed. at 35 went. in 1 cm.sl.**	**Content in %,**				**The residual content of the solvent,%**
				Phospholipids	**Free gossypol**	**Bound Gossypol**	**The total content of tocopherols, mg 100 g**	
1.	4.2–5.8	0.22–0.26	34–41	0.7–0.9	0.13–0.22	0.16–0.28	70–80	traces
2.	6.1–7.6	0.26–0.30	46–52	1.3–1.6	0.27–0.38	0.30–0.43	60–70	traces
3.	7.9–12.3	0.34–0.35	not super-vised	1.9–2.6	0.45–0.55	0.50–0.61	50–90	traces
4.	12.6–14.8	0.36–0.41	not super-vised	2.0–2.8	0.60–0.70	0.75–0.93	40–50	traces

Evaluation of technological methods of purifying raw cotton oil suggests that the quality and nutritional benefits of refined oil mainly depend on the content of free fatty acids, phospholipids, gossypol and its derivatives, as well as other substances. The reduction and complete removal of some oil-related substances can significantly improve the performance of the final product. Purification of raw oil and ensuring high levels of final products also depend on the nature of the raw materials and methods of producing cottonseed oil [3,4]. When processing raw cottonseed oil with an alkaline solution of sodium aluminate of various concentrations, the raw materials are partially neutralized and some of the associated substances are removed.

The most significant decrease in the content of free fatty acids and related substances is observed at an alkali concentration of 15%.

When this is achieved by improving the color of the partially neutralized cottonseed oil. The most acceptable technological data is obtained by partially neutralizing raw cottonseed oil with an initial acid number of not more than 4.1 mg KOH / g. This suggests that alkaline solutions of sodium aluminate exhibit their reactivity to a certain level of acid number and the content of substances accompanying the original oil [3].

For the first time, compositions of adsorbents from local materials were created for the purification of cotton fat from the residues of gossypol and its derivatives, catalyst metals and other impurities. Technological regimes have been developed for the transesterification of high-melting cotton fat with rosehip oil and corn germ, which makes it possible to obtain suppository bases of the required quality [4]. Thus, the optimal technological conditions for the refining of crude oil using the recommended new technologies were determined, and the possibilities for increasing the yield and quality of refined oil were established.

The technological parameters have been established, which allow to significantly reduce the content of substances accompanying the oil and improve its color.

The chemical interactions of the main components of crude oil with an alkaline solution of sodium aluminate are determined and their correspondence with known chemical phenomena is established.

A technology is proposed to intensify the partial alkaline neutralization of raw cotton oil with a solution of sodium aluminates activated by treatment in an electromagnetic field.

The technological parameters were optimized and the modes were determined to improve the quality of partially neutralized oil.

Obviously, the final process of alkaline refining of raw materials with low acid number and improved color can be reduced by reducing the consumption of sodium hydroxide, which increases the yield of refined oil and improves its quality.

References:

1. Harutyunyan N. S. and others. Technology of processing fats. – M .: Pishepromizdat. 1999.
2. Ilyasov A. T., Serkaev K. P., Vakhabova D. Z. Fractional refining of cottonseed oil // Fat-and-oil industry. 1999. – No. 4. – P. 30–31.
3. Abdurakhimov. Investigation of the influence of heterogeneous nickel catalysts on the process of liquid-phase hydrogenation of fats and fatty acids Abstract. Diss., Dr. tech. Sciences.– Tashkent, 1975. – 55 p.
4. Mazhidov K. Kh. Research and improvement of the technology of hydrogenation of cotton oil on modified alloyed stationary catalysts. Author. Diss., Doctor of Engineering. Science-L. VNIIZh 1989.– 54 p.

Hujakulova Dilbar Jurakulovna,
Majidov Kaxramon Halimovich,
Bukhara engineering-technological institute,
Republic of Uzbekistan
E-mail: kafedra-03@mail.ru

TECHNOLOGY OF DEODORIZATION OF SOYABEAN OIL

Abstract. The technology of deodorization of local soybean oil has been studied. Soybean oil is obtained from soybean seeds grown locally. For deodorization, oils were obtained under production conditions. Studies conducted in laboratory and production conditions. The effect of pressure, temperature and duration of the deodorization process on the quality indicators of deodorized oil has been studied. Equipment and technological lines for the deodorization of local varieties of soybean oil have been selected. Research in production tests carried out on a bubbling device consisting of tubes with holes for bubbling steam into oil. To maintain absolute pressure during deodorization, steam ejector vacuum systems were used. The effectiveness of such systems on soybean oil ranged from 75 to 95%. Distillates deodorization ranged from 0.25 to 0.50% of the raw materials supplied to the deodorizer. In experiments, tocopherols and sterols were isolated from the distillate and fatty residue of water from a barometric condenser. The use of tocopherols as food antioxidants was carried out by comparison with other food and synthetic products. The results obtained ensured an increase in the quality and perfection of the technological processes of deodorization of soybean oil.

Keywords: Local soybean oil, deodorization technology, laboratory and pilot plants, technological regimes, quality and physical-chemical characteristics of deodorized oil, deodorized oil distillates and their use.

Deodorization is an oil treatment process with steam, in which good quality steam, obtained from deaerated and properly treated water, is injected into soybean oil at low absolute pressure and high enough temperature to distill off free fatty acids (FFA) and odorizing substances and separate these volatile substances from the oil flow [1–3].

The role of deodorization in obtaining and refining of food fats and oils is that deodorization is the last stage of the preparation of oil for use as an ingredient in margarines, shortening, salad oils, frying oils, confectionery fats and many other foods [4–5]. Deodorized oil can be considered as ready for various classification parameters, depending on the characteristics and tastes of the consumer market of a particular region or country. In some regions they like oil with pronounced taste and smell, in others they prefer oil with characteristic color [6].

Studies of the technology of deodorization of soybean oil, obtained based on soybean seeds, are of both scientific and practical interest.

Soybean oil was deodorized in a laboratory setup.

To analyze the composition of the original and deodorized soybean oils, modern methods of physical-chemical research were used [7; 8].

The quality indicators and the fatty acid composition of the initial and refined samples of local varieties of soybean oils are given in (table 1).

The intervals of variation of the working parameters of the process of deodorization for the production of high quality oils given in (table 2).

Table 1. – The composition of raw and refined local varieties of soybean oils

Components	Crude oil	Refined oil
Triglycerides	95–97	More than 99
Phosphatides	1.5–2.5	0.003–0.045
Unsaponifiables:	1.6	0.3
Plant Sterols	0.33	0.13
Tocopherols	0.15–0.21	0.11–0.018
Hydrocarbons (squalene)	0.014	0.01
Free fatty acids	0.3–0.7	Less than 0.05
Traces of metals, mg / kg:		
iron	1–3	0.1–0.3
copper	0.03–0.05	0.02–0.06

Table 2. – Soybean oil deodorization conditions

Absolute pressure, mm hg	1–6
Temperature, °C	252–266
Duration of exposure, min	15–16
Stripping steam, % of oil mass	1–3

The effect of each parameter on the deodorization process is studied.

Pressure does not have a perceptible effect on quality if the deodorizer operates at an absolute pressure in the range from 1 to 6 mm hg. It is established that pressure is higher than 6 mm hg even in the range of 7 to 9 mm hg will lead to problems with quality, such as the appearance of undesirable taste and smell.

Deodorization temperature is a parameter that can be considered as variable. It directly affects the vapor pressure of volatile components that must be removed. By increasing or decreasing the temperature, one can achieve a correspondingly lower or higher rate of removal of odorizes.

The duration of exposure during deodorization is the time during which the raw material is at the deodorization temperature and at a given flow rate of bubbling steam. The effectiveness of bubbling depends on the ability of the devices to thoroughly mixing steam and oil. In modern equipment, the duration of exposure is from 15 to 60 minutes. This time refers to the oils entering the deodorization after chemical (alkaline) refining and with a FFA content of less than 1%.

To obtain the highest quality deodorization product, it is necessary that the raw materials are also of better quality. Improper or inadequate processing at any stage of the process can lead to a change in quality and even to permanently spoiled oil entering into deodorization.

Soybean oil contains about 0.1% tocopherols, and at a deodorization temperature of 260 to 265 °C, from 40 to 50% of this amount will be removed.

By-products of deodorization of soybean oil consist of a mixture of phosphatides, unsaponifiable substances, free fatty acids and soap.

The value of each by-product depends on its composition.

Distillates of deodorization range from 0.25 to 0.50% of the raw materials fed to the deodorizer. They consist mainly of unsaponifiable substances and some fatty acids. Distillates of deodorization are volatile organic substances released as a valuable by-product in soybean oil deodorization (Table 3).

Table 3.– Distillates of deodorized soybean oil

Component	Molecular weight, g / mol	Relative volatility
1	*2*	*3*
Fatty acid	280	2.5
Squalene	411	5.0

1	*2*	*3*
Tocopherol	415	1.0
Sterol	410	0.6
Sterol ester	675	0.038
Butter	885	Insignificant

The recovery efficiency of distillates of deodorization is very high. In experiments, tocopherols and sterols were recovered from distillate and from the fatty residue of water from a barometric condenser. 98% of tocopherols and more than 95% sterols were recovered from the distillate.

In (table 4) is shown that soybean distillates contain 18% sterols, of which 44% is stigmasterol. The approximate composition of the sterol components of soybean oil is as follows: 20% campestero l.20% stigmastero l.53% *β*-sitostero l.4% *δ*-avenasterol and 3% δ-stigmasterol.

Table 4. – Composition of distillates of deodorization of soybean oil,%

Components	**Soybean oil**
Non-pollinated substances	33
Tocopherols	11.1
α – tocopherols	0.9
Sterols	18
Stigmasterol	4.4

Sterols are used in production of pharmaceuticals

Soybean oil is characterized by a special chemical composition. Soybean oil with such chemical composition is easily subjected to deodorization technology. In deodorization of soybean oil distillates containing in its composition substances with functional properties are obtained.

References:

1. Arutyunyan N. S., Kornena E. P., Yanova L. I. and others. Technology of fat processing. – M.: Pishepromizdat, 1999.– 452 p.
2. Тютюнников Б. Н., Гладкий Ф. Ф. и др. Химия жиров. – М.: Колос, 1992.– 448 с.
3. Тютюнников Б. Н., Науменко П. В., Товбин И. М., Фаниев Г. Г. Технология переработки жиров. – М.: Пищевая промышленность, 1970.– 652 с.
4. Sonntag N. O. V., in World Conference Proceedings Edible Oils and Fats Processing, Basic Principles and Modern Practices, edited by D. R. Erickson. American Oil Chemists' Society, 1989. – P. 406–411.
5. Boyer M. J., in Proceedings: World Conference on Emerging Technologies in the Fats and Oils Industry, edited by A. R. Baldwin. American Oil Chemists' Society, Champaign, IL, 1986. – P. 149–154.
6. Руководство по методам исследования, технохимическому контролю и учету производства масложировой промышленности.– Л.: – Т. III. 1964.
7. Арутюнян Н. С., Аришева Е. А. Лабораторный практикум по химии жиров. – М.: Пищевая промсть, 1979.– 176 с.
8. Руководство по методам исследования, технохимическому контролю и учету производства масложировой промышленности.– Л.: – Т. VI. – Кн. 1–2. 1974.

Section 3. Technical sciences

Gulamova D. D.,
Institute of Materials Science (SPO)
"Physics – Son" of Academy of Sciences of Uzbekistan,
Tashkent Uzbekistan

Kurbanova A. Dj.,
Tashkent Institute of Irrigation and
Agricultural Mechanization Engineers (THAME),
Tashkent, Uzbekistan

Komilov Q. U.,
Tashkent Institute of Irrigation and
Agricultural Mechanization Engineers (THAME),
Tashkent, Uzbekistan
E-mail: kaypara@list.ru

RECEPTION WITH SOLAR ENERGY AND STUDY OF PHASE COMPOSITION OF HIGH-TEMPERATURE SUPERCONDUCTORS HOMOLOGOUS SERIES $Bi_{1,7}Pb_{0,3}Sr_2Ca_{(N-1)}\ Cu_NO_Y$ (N = 3–20)

Abstract. The effect of solar radiation on the formation and properties of high-temperature superconducting phases of homologous series $Bi_{1,7}Pb_{0,3}Sr_2Ca_{(n-1)}\ Cu_nO_y$(n = 3–20) is researched. The dependence of the completeness of HTSC phase synthesis on time-temperature conditions within the range of 846–848 °C. 3–120 hours. The formation defined ≈ 90%, in 2223 and 2234 phases. The synthesis under the influence concentrated solar radiation allowed to obtain stable high-temperature superconducting materials with Tc > (107 ÷ 151) K. The prospects for the use of solar technology is determined for the synthesis of a number of high-temperature superconductors Bi1,7Pb0,3Sr2Ca(n-1) CunOy (*n* = 3–20).

Keywords: solar radiation, high-temperature superconductors, HTS materials.

Introduction

High-temperature superconductors based on the system Bi-Pb-Sr-Ca-Cu-O constitute a homologous series represented by the formula $Bi_{1,7}Pb_{0,3}Sr_2Ca_{(n-1)}\ Cu_nO_y$. There are relatively detailed studies on conditions of synthesis and properties of HTSC that start from the beginning of this series *n* = 1–4, and very limited information on properties of HTSC phases with n > 4. Revealed direct correlation between the increase in the critical transition temperature to the superconducting condition T_c and increase in "n" for a raw $Bi_{1,7}Pb_{0,3}Sr_2Ca_{(n-1)}\ Cu_nO_y$ (*n* = 3–20) allowed to assume the possibility of formation of HTSC phase with a T_c 107K [1]. The conditions for

the synthesis have a decisive influence on the critical properties of high-temperature superconductors. The most common method of synthesis of high-temperature superconductors in the solid phase has significant limitations imposed by the diffusion mechanism of interfacial interactions [2; 3]. Wider possibilities and advantages of melting techniques offer the prospects for finding new technological solutions based on the melted synthesis, that can lead to an increase of critical transition temperature to the superconducting condition and the critical amperage [4]. The increase in T_c can be solved at the expense of a different, compared to the solid phase, phase formation and the nature of the interfacial interactions in the melt and the subsequent reactions in the solid phases during the formation of the target high-temperature superconducting phases. In addition, the reasonable expectation to increase the critical current opportunities lie in the texture and morphology during melt processing control, for example by creating high temperature gradient during the cooling procedure of the melt.

In order to obtain a melt as a heating source high frequency currents are used, induction currents, resistance currents, laser, radiant flux, generated by mercury and xenon lamps [2–4].

Data on the comparative analysis of the impact of spectrum from heating sources on the properties of the materials being processed are very limited, the photosynthesis of inorganic materials are rarely used and specific explanation of the effect is given in [5]. The energy consumption of the heating sources to achieve high temperatures in technological processes under the severe power constraints makes important to appeal to the study of the possibility of using renewable natural sources of energy, including solar radiation. The possibility of using solar radiation for the synthesis of the inorganic materials has been studied in [6].

The positive change of the properties is found and the prospects for use of solar radiation for the synthesis of oxide materials is determined, including a higher fire resistance of complex compositions. However, the explanation of the results of the influence of the solar spectrum on the nature of the formation, interaction phases and properties of the target materials mainly were tentative.

The [7; 8] under the explosion of concentrated solar radiation the synthesizeation of titanates of pseudobrookite type, mono- and di-lanthanide titanate РЗЭ (РЗЭ = La-Lu), fluorite solid solutions based on ZrO_2, HfO_2 the properties of these materials investigated. The distinctions of properties if these materials is defined that synthesized under the influence of solar radiation received by other methods. The changes of the properties allegedly explained by the influence of the solar spectrum on the polarization of the valence electrons and the influence of "nadstehiometrichnogo" oxygen.

Based on these results and the benefits of using concentrated solar radiation as a heating source, inorganic materials synthesis experiment under the influence of solar radiation was distributed to receive high-temperature superconductors homologous series of raw $Bi_{1,7}Pb_{0,3}Sr_2Ca_{(n-1)}Cu_nO_y$ (n = 3–20).

Experiment

The synthesis and the study the properties of the precursors and HTSC of the ceramic series $Bi_{1,7}Pb_{0,3}Sr_2Ca_{(n-1)}Cu_nO_y$ c (n = 3–20). Synthesis of precursors for nominal compounds $Bi_{1,7}Pb_{0,3}Sr_2Ca_{(n-1)}Cu_nO_y$ (n = 3–20) was carried out by quenching of the melt obtained under the influence of solar radiation and solar radiation simulators at a density ≈ 680–750Вт/см^2 (*SFAQ*-method)[9]. Superconducting ceramic is obtained on the basis of glass-ceramic precursors obtained by ceramic technology. The microstructure and phase composition was examined under the electronic microscopes "NEOPHOT NU-2" Model JEM-1200EX11, JEOL Co., Ltd., Tokyo, Japan, the X-ray diffractometer DRON-UM-1 (CuKα-radiation, Ni-filter).

Phase composition of precursors of the following denominations $Bi_{1,7}Pb_{0,3}Sr_2Ca_{(n-1)}Cu_nO_y$ (n = 3–20) in the initial state is represented by the diffraction patterns (Fig. 2a). The weak diffuse reflexes of pre-

cursors with "n = 3–5" more clearly manifested when "n > 5". Increase "n", so to say elevated levels of CaO and CuO, leading to destabilization of the glass phase.

After annealing at 500 °C, 3h. the diffraction patterns of ceramics denominations $Bi_{1,7}Pb_{0,3}Sr_2Ca_{(n-1)}Cu_nO_y$ (n=3–5) much broadened reflexes phase of 2201 existed: (Figure 2a). In addition, the part of the weak intensity reflexes is defined, which could be attributed to the phase (2212). After annealing at 600 °C, 3h. the phase (2201) was better crystallized and clearly manifested phase appeared (2212). In addition to the reflections belonging to (2201) and (2212) phases, there were a small number of low-intensity reflections present: $2\theta_{CuK\alpha}$ (20,9; 28,4; 30,1; 36,8; 37,2; 38,2 and unknown phases (X phases), which did not correspond to the phases of 2223, 2234 and the intermediate phases that are involved in the formation of HTSC phases formation reactions at the solid-phase synthesis by [10].

With an increase of the annealing temperature to 700 °C., 3 h. the (2201) phase disappeared; the main phase was (2212) and (2223) phase was present at small portions. With an increase of the annealing time increased to 20 hours the 2212 phase contents increased. Annealing at 845–848 °C, 60–100 h. allowed to obtain ≈90% of the mixture ≈ HTSC phases (2223) and (2234). The selection of phase (2234), and to determine its amount was difficult because of the close values of 2θ° of these phases. The content of (2212) phase decreased with increasing in annealing time to ≤ 10%. The characteristic features of the heat-treated samples were a series of reflections corresponding to 2223, 2234 and, perhaps other phases of HTSC-homology with the unit cell parameters phase identified according to data [11; 12] in assumption of (2223): a = 5.2832–5.3539; b = 5.3698–5.5075; c = 36.506–37.3855; (2289): a = 5.0545–5.1226; b = 5.6696–5.8918; c = 36.4798––37.2383.

The formation of mixtures of homologous phases obtained in the samples synthesized by the (SFAQ) – method, is not established in the synthesis method of solid-phase reactions. When a solid phase synthesis method is used the superconducting phases are formed by diffusion reactions between 2201 (2212) and intermediates junctions. In the synthesis of the precursors obtained under the use of (SFAQ) – method under the influence of solar radiation, it can be assumed that the rapid quenching of the melt "freezes" existing clusters in the melt cluster-germs of the basic **perovskite** structure of different stoichiometry. On the basis of these embryos in the heat treatment of precursors the HTSC phases homologues are formed.

The effects of formation of phase-homologues were noted previously in synthesized by the use of the same method of fluorite-type solid solutions on the basis of ZrO_2(HfO_2) and **РЗЭ** titanate pyrochlore, [7–9]. Probably, the formation of a series of phase-homologues inherent to defect in the crystal structure and their formation involves both the "excess" oxygen and affects of the excited state of electrons that occurs due to the exposure to the melt of the concentrated radiant flux.

The microstructure of the superconducting ceramic compositions had the superconducting material's characteristics lamellar structure (Figure 3). All ceramic compounds under the research had Meissner effect to 184K, that is confirmed by X-ray diffraction data.

Conclusion

Synthesis under the influence of the concentrated radiation allow to obtain stable high-temperature superconducting materials with T_c > 107K.

The lack of intermediate phases, which, according to the solid-phase synthesis 2212, 2223, 2234 phases should take part in their formation, allow to assume formation of different from the solid-state mechanism of HTSC phases of the precursors synthesized under the influence of concentrated solar radiation. The conditions for synthesis are defined in the rapidly melting gradient conditions. The rapid quenching of the melt "freezes" different on the stoichiometry

"germs" on the basis of which the heat treatment of superconducting phases are formed from the series of homologs $Bi_{1,7}Pb_{0,3}Sr_2Ca_{(n-1)}Cu_nO_y$ (n = 3–20). These phases can be noted on the diffractograms with the groups of reflexes corresponding to HTSC phases with different parameters of the unit cell.

The formation of the superconducting phases not only in ceramics but also in precursors suggests the following mechanism, which involves the formation of the clusters – "embryos" in the melts with the compound composition and crystalline structure, close to the most stable compound structure in 2201 and part of the germs, representing the base that participates in the formation of the structure of high-temperature superconducting phases. The differences of stoichiometric clusters – "germ" is influenced by the conditions of synthesis, characterized by a sharp temperature gradient in the melting and quenching the melt.

Melting in gradient temperature conditions can lead to the formation of a melt-homologues clusters of various compositions, which are fixed with melt quenching. These results indicate the possibility of a new "green" synthesis technology of HTS materials.

References:

1. Tarascon J. M. et al., // Phys. Rev B37, 9382 (1988).
2. Gopinath S. S. Bi-Sr-Ca-Cu-O Thin films grown by flash evaporation and pulsed laser deposition // Thesis Submitted to Texas A&M University in partial fulfillment of the requirements for the degree of Master of Science. Texas, December, 2003.
3. Tretyakov Y. D., Kazin P. E. New challenges and solutions in material ceramic superconducting cuprates. // Inorganic Materials, 1993. – T. 29. – No. 12. – P. 1571–1581.
4. Acrivos J. V., Chigvinadze J. G., Gulamova D. D. Bond resonance and superconductivity in (Bi1.7Pb0.3Sr2Can-1CunO2n + 4 + δ)2. // International Conference Superconducrivity and Magnetism, Turkey, – Istanbul, in 2012. – 29 April-4 May.
5. Chigvinadze J. G., Iashvili A. A., Machaidze T. V. On the Possibility of Observation of the 3D-2D Phase Transition in Vortex Lattice of Layered High-Temperature Superconductors of BSCCO ($Bi_{1,7}Pl_{0,3}Sr_2Ca_2Cu_2O_4$) // Phys. Lett. A. 2002. – V. 300. – P. 524–528.
6. Gulamova D. D, Ismailov T., Turdyev D. Zh., Aralov Kh., Zufarov M., Uskenboev D. Influence of concentrated solar radiation on the properties of oxide systems // Renewables and geliomaterialovidenie. Proceedings of the International Conference. 29–30 September. – Tashkent, 2005. – P. 184–185.
7. Gulamova D. D., Suleymanov S. Kh., Azimov S. A. The study of ternary systems ZrO_2-R_2O_3-$R^1{}_2O_3$, obtained in a solar oven. Conference: The use of solar energy, Katsiveli, 1981. – P. 56–59.
8. Gulamova D. D. Effect of Concentrate Solar Energy on the Properties of Oxides // 8th International Symposium On Conc.T echnol., 1999. – Koeln, Germany.
9. Tyson K., Kmiec J., Acrivoc J. V., Gulamova D. D. and Chigvinadze J. G. Bond resonance in superconducting rapid cooled alloys: $(Bi_{1,7}Pb_{0,3}Sr_2Ca_{n-1}Cu_nO_{2n+4+\delta})_{2,\ n=1\ to\ 9}$ detected by novel local atomic enhanced XRD // National ACS Meeting San Diego, CA March 2012. – V. 58. – P. 23–24.
10. Yoshihiro Abe. Superconducting glass-ceramics in BiSrCaCuO. Production and its Application // 1997. (Nagoya Institute of Technology, Japan). – P. 25–44.
11. Private Communication, primary reference: Michel C., Hervieu M., Grandin A., Deslandes F., Blagochinniy t, J., Ravo B. de la Matiere et du Rayonnement, Caen, France. 1988.
12. Chin. Sci. Bull., – V. 35. – 573 p. 1990. Primary reference: Shi, North Carolina, Shi F., Ma Z.-S., Wang X.- f., Rong T.S., Du J. Zhou.

Rasulov F. R.,
Ph. D., dos.
Mamedov A. T.,
Doctor of Technical Sciences, prof.,
Azerbaijan Technical University, Baku
E-mail: resulovfr@gmail.com, arif-1947@mail.ru

FORMİNG CHEMİCAL COMPOSİTİON OF COATİNG ON THE İRON CASTİNG

Abstract. The mechanism of formation of chemical microheterogeneity of metal of a composite covering of cast iron casting is studied. It is established, that formation of structure and properties composite covering of cast iron casting depends as on chemical and fractional structure of a powder and a thicknes of its layer and a temperature condition of impregnation powder liquid metal.

Keywords: coating, casting, impregnation, powder spread, alloy.

1. Introduction. Structural changes in the crystallization of liquid iron, penetrating into the pores of powder spreading, occur as a result of the interaction of the melt with particles of the powder of the composite coating. At the first moment after wetting the surface of the powder particles of the spreading with coasting iron, a surface chemical reaction takes place between them, the speed of which depends on the state of the surface, the temperature in the joint zone and, above all, the heat of formation of the forming compound and is determined by the diffusion laws. The second stage is the dissolution of the metal particles in the melt. The formation of the solid solution and the intermetallic phases and the dissolution of the solid metal proceed simultaneously. Therefore, undoubtedly, the final structure will depend on the ratio of the rates of these processes. At the same time, directly in the contact part of the the powder particle paste with liquid iron, when the particles are completely melted, these changes are associated with the extraction of excess heat from the melt to heat and melt them. In the middle and peripheral parts of the spreading layer, the powder particles are partially dissolved in the cast iron. The reasons for this should be sought in the results of the heterophase interaction of the powder particles with the binding melt. Therefore, issues related to the formation mechanism of the phase "particle boundary – metal", the near-contact zone, the severity of chemical and phase microheterogeneity of the composite metal, become of paramount importance. It is also important to ascertain the actual value of the degree of crystallographic affinity for the structural changes occurring in the binder metal under the influence of the alloy of the particles of powder spread.

It is known that in the pulverized powder of the CrNi80SiB3 alloy nickel in the overwhelming majority is in the boride (Ni_3B) and in silicide (Ni_3Si_2), and chromium is in the boride (CrB) and in carbide (Cr_7C_3) phases.

2. Discussion of the results. The metal of centrifugally cast castings of bushings with dimensions of 100 × 43 × 180mm (100-outer diameter; 43-wall thickness; 180-height) with powder paste thickness x_n = 5; 10 and 15mm alloy CrNi80SiB3 – gray cast iron.

As a result of the impregnation of cast iron in the layer of powder spread, the dispersion of the structure and chemical heterogeneity of the binder metal significantly increased. The change in the thermal conditions of the formation of the periwinkle structure was also reflected in the nature of the distribution of the excess phase; an uneven, but dispersed precipitation of which

inside the grain and along its borders in the experimental metal contrasts with coarse local precipitates in the intergranular region in the metal of the control castings. Undoubtedly, these changes were the result of not only intensive heat exchange between the liquid metal and the powder particles of the spreading. The temperature conditions of the casting and the physicochemical constants of the selected powder materials ($T << T_{mt} > T_p$, where T_{liq} is the liquidus temperature of the alloy, T_{mt} is the melting point of the powder material, T_p is the pouring temperature of the alloy) powder in the crystallized solid solution as a separate phase [1].

Thus, the powder particles also play the role of refractory inoculators, whose catalytic influence on the process of forming the crystal structure of the alloy is largely determined by the degree of their crystallographic means with the matrix of the binder metal. Therefore, of particular interest is the analysis of the causes of structural changes under the influence of non-isomorphic powder particles with a significant discrepancy between crystallographic parameters (cast iron Class 15 $\alpha = 2.8657$ Å ; alloy of the powder = 3.5926 Å)

The mechanism of influence may be associated with a decrease in the work of the formation and growth of crystals of the bonding alloy on the finished interface. As a result of high temperature, a regular the crystalline-structured transition zone is made on the contact between the surface of the powder particle and a crystallizing melt.

However, the reduction of the heterophase interaction only to the appearance on the surface of the powder particle of a spreading of the boundary zone with a different crystallographic orientation without taking into account possible changes in its chemical composition and uniformity of the particle material is schematic.

Further study of this issue confirmed the need for a deeper analysis of the phenomena in the contact zone. Thus, the observation of partially dissolved powder particles by means of color etching revealed heterogeneity of their color coloration, varying from yellow – brown (corresponding to the solid solution) to green and burgundy. In addition, each color region has a clear boundary.

Colors of inhomogeneity are accompanied by different values of microparticle, the natural difference between which between the matrix and particle is complemented by an anomaly inside the particle itself in accordance with the colored areas.

The values of microparticle H_μ, MPa:

matrix metal binder 2140–2190
matrix (near the contact zone) 2140–2920
contact area.....3490
inner powder boundary.....2070
powder core 1250

Such a distribution of microparticles is a consequence of the chemical heterogeneity of the particle and the area attached to it. This assumption is fully confirmed by the results of micro X-ray spectral analysis.

In the initial state, powder spreading alloy CrNi80SiB3 consists of 78–80% Ni; 15–17% Cr; 3% B; 0.2–0.3% C; 0.7–1.2% Mn; 1% Si; 0.75% P and 4.5% Fe, after crystallization interaction with a binder melt of gray iron of composition (Class 15) contains more carbon and iron with decreasing Ni and Cr (Fig. 1).

The type of curves of the contact layer of the partially dissolved powder microparticle components of the bases (Ni and Cr) indicates the different intensity of its flow and allows you to clearly distinguish the contact layer, the core of particles and determine their sizes (particle size distribution of powders corresponded to fractions: + 50–60; + 63–100; + 100–160; 160–200 and 200–315 μm). The change in the chemical composition of the microparticles of the powder and the contact layer has a diffusion origin [2].

The contact layer around the particle with a clearly defined boundary indicates the probability of formation of intermetallic phases by the mechanism of reactive diffusion.

Taking into account the aggregate state of the interacting particles of the powder and the bonding

alloy, we can assume that new phases is formed simultaneous dissolution of the microparticle in the liquid metal and chemical reaction at the interface, the speed ratio of which regulates the formation of a particular phase.

Under real conditions of joint crystallization of the melt with a solid multi-component particle, the variable ratio of the melt, the degree of crystallographic affinity between the matrix and the particle, and finally, the change in the value of the solubility of the alloy components of the solid particles with simultaneous alloying or crystallizing binder were reflected in the ratio of the rates of these processes.

Taking into account the amount of alloying components in the powder particle from alloy CrNi80SiB3 and the fact that elements participating in the diffusion process can form intermetallic compounds, it can be assumed that a complex chemical Laves phase forms in the contact layer.

The presence in the binder metal of dispersed particles of variable chemical composition and with a diffusion interlayer of a certain width from intermetallic strengthening phases that differ from the base metal of particles and cast iron in the type and parameters of the crystal lattice ($\alpha_{phase} = 4.74$ Å) explains the increased heat resistance of the test metal [3].

When reducing the powder coating layer thickness from 15 to 10 and 5 mm, as well as increasing the pouring temperature from 1360 to 1440 °C, the degree of dissolution of the powder particles in the cast iron of the bundle increases and the segregation of Ni, Cr, Si and P over the cross section of the composite coat casting decreases.

By chemical analysis of the metal over the cross section of the manual, it was established that the smaller the thickness of the powder coating, the greater the degree of uniformity of the distribution of Ni, Cr, Fe, and C across the coating thickness of the iron casting. So, with an increase in the thickness of the spreads made from the powder of the alloy $CrNi80SiB_3$ from 5 to 10 and 15 mm, the content of the elements changes from the surface to the contact zone; namely: nickel decreases from 45.1; 55.1 and 60.2% to 44.0–44.2%, and chromium from 11.0; 14.5 and 15.2% to 9.4–9.8%, the iron content increases from 44.5–40.2 and 38.5% to 46–46.7%, and carbon content with 1.47; 1.29 and 0.96% to 1.75–1.80% [4] (Fig. 2).

The degree of saturation of liquid iron, poured into the mold at 1440 °C and penetrated into the pores of the powder composite with elements of the CrNi80SiB3 a coasting coat alloy of casting 43 mm thick, is shown in the (table 1).

Table 1. – Changes in the chemical composition, cast iron ligaments depend on the thickness of the composite coating

Thickness	**Number of elements,%**				
Powder coating, mm	**Powder mm in alloy**	**Composite coating on iron casting**			
		Ni	**Cr**	**Si**	**P**
5	Ni = 78–80 Cr = 15–17 Si = 1 P = 0.75	9.64 / 17.14	2.20 / 3.24	2.20 / 2.32	0.43 / 0.34
10		4.25 / 14.34	1.95 / 2.98	1.96 / 2.32	0.59 / 0.37
15		3.09 / 13.42	0.89 / 2.84	1.94 / 2.34	0.63 / 0.39

Note: In the numerator – at the surface; in multipliers – at the contact area

As can be seen, the nature of the dissolution of particles and the diffusion of Ni; Cr; Si and P in the cast iron of the ligament at the surface of the coasting coat of the casting significantly depends on the thickness of the powder coating, and the content and distribution of these elements in the zones varies significantly. So,

in experimental castings with a total thickness of 50 mm in the surface zone of the gearbox, an increase in the thickness of the powder spreads from 5 to 10 and 15mm led to a decrease in the content of elements of the $CrNi80SiB_3$ alloy in thin interparticle interlayers of cast iron: 9. 64% at 4.38 and 6.51%; for chromium, from 2.20% to 0.25 and 1.31%, and for silicon, from 2.20% to 0.34 and 0.36%. Then as the phosphorus content in the pig iron impregnated in the porous spread increases from 0.43% to 0.51 and 0.63%, while in all cases of the casting with the impregnation of the powder spread the metal of the contact gearbox itelno increasingly complex is saturated with Ni, Cr and P than in the peripheral regions [4; 5].

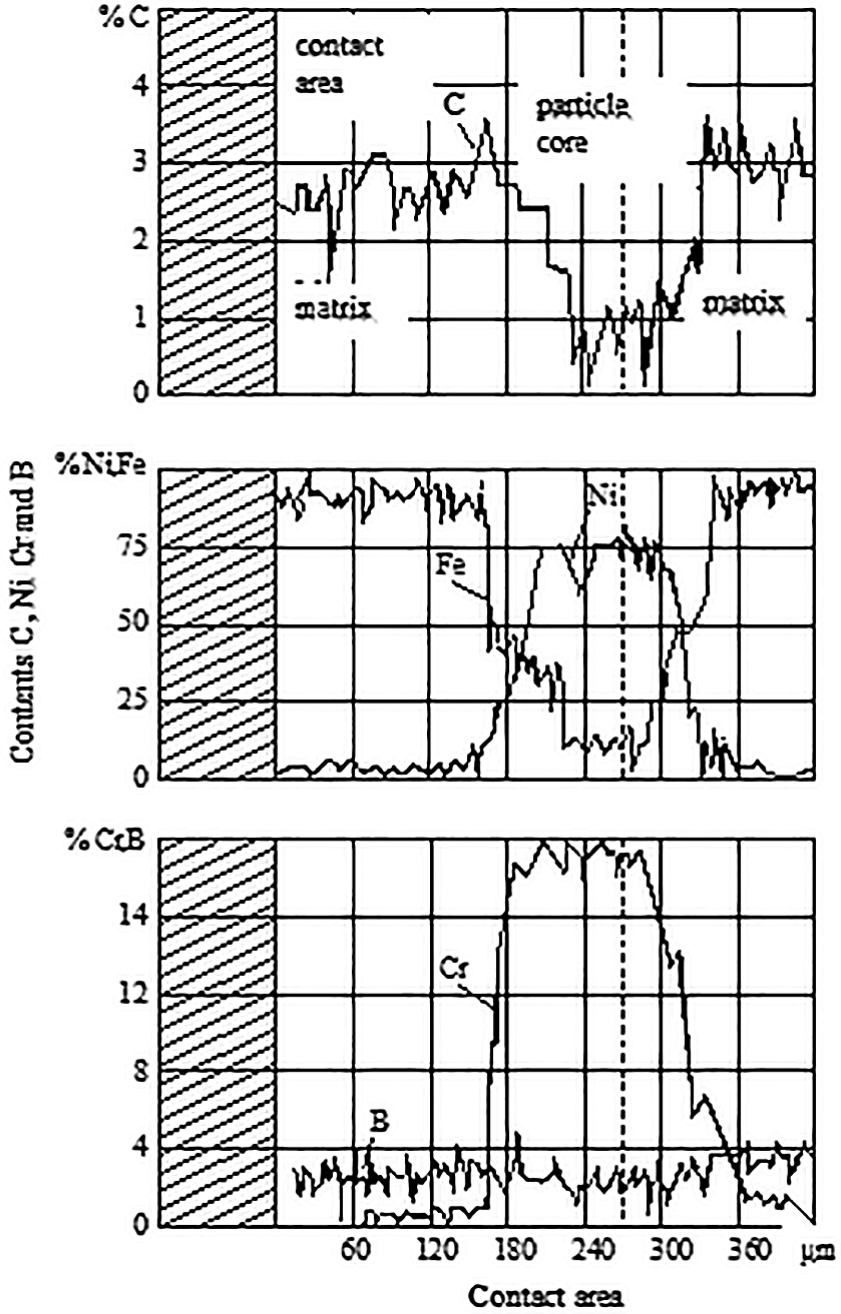

Figure 1. Chemical Inhomogeneity of Spray Particles from alloy CrNi80SiB3 and the adjacent area

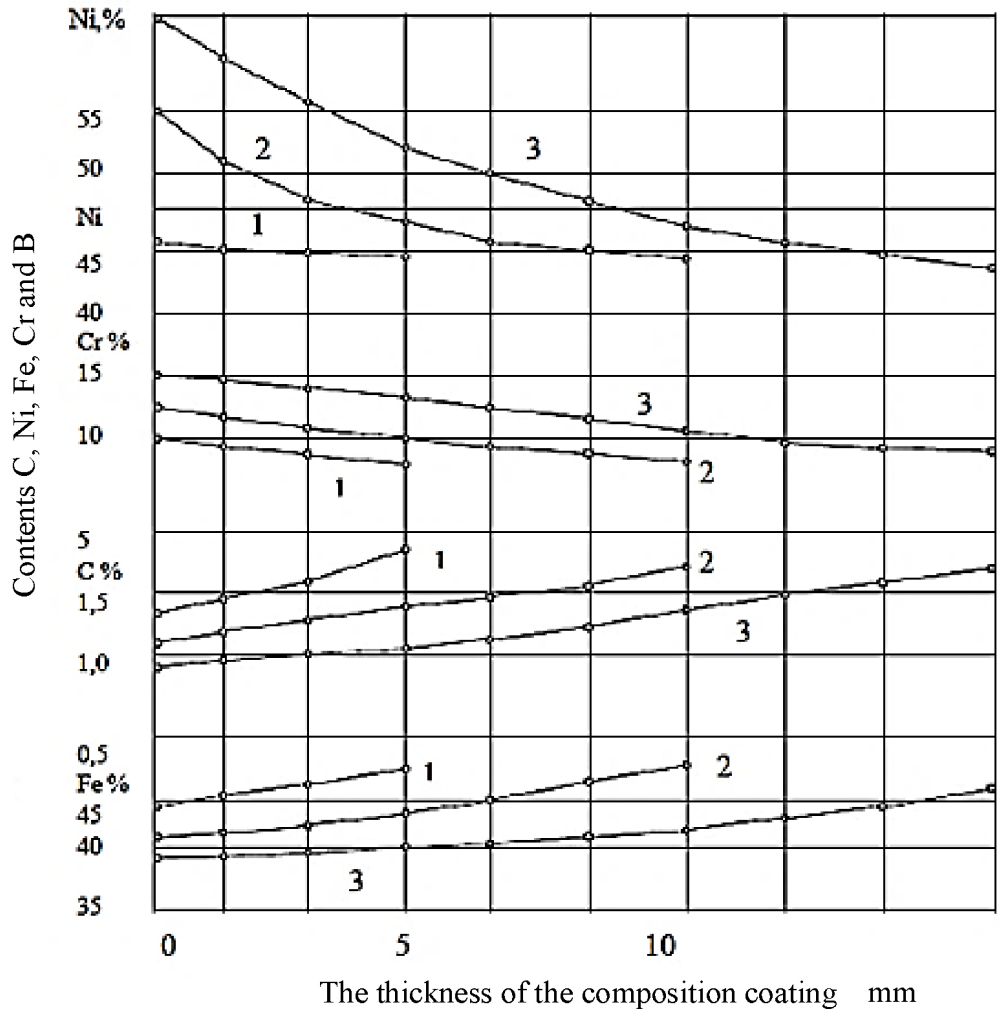

Figure 2. Changes in the chemical composition of the gearbox of the casting "powder coating of alloy CrNi80SiB3 – cast iron Class 15" depending on the thickness: (figures on the curves) of spreading: 1, 2 and 3 – thickness of powder coating of 5, 10 and 15 mm, respectively; T_p = 1440 °C, δ = 43 mm

At the same time, the solubility and diffusion of elements from solid particles of the powder alloy into the cast iron of the bundle is much greater than in the surface zone of the coasting coat. However, with an increase in the thickness of the spread, the content of the elements that become bonded to the cast iron composition decreases as much as in the metal surface zones of the gearbox, namely, as the thickness of the spread is increased from 5 to 10 and 15 mm, the content of Ni and Cr decreases by 2.80 and 3.72%, 0.27 and 0.40%, respectively;

Regardless of the thickness of the powder spread in the metal of the contact zone, the silicon content remains almost unchanged; while the phosphorus content in comparison with the initial amount (0.7––0.8%), decreases almost 2 times and is 0.35–0.38%.

A coasting coat of iron casting is characterized by a layered structure, which depends on the melting temperature and the degree of interaction, the particle size distribution of the powder particles, the thickness of the spreading layer of the melt impregnation temperature of the matrix during the casting process. Part of these parameters in the casting process is maintained very approximately and cannot be strictly controlled. Since the moment of contact of liquid iron with powder spreads made from alloy CrNi80SiB3, some of

the powder particles are dissolved in the hardening cast iron and are doped with Ni and Cr. This process proceeds most efficiently, directly in the contact zone and near-contact interlayers, both on the side of the powder layer and the wall of the casting.

These elements affect the formation of the metallic base and the shape of gray cast iron graphite in different ways: Ni and Mn have austenitizing effects and contribute to the formation of lamellar graphite; Cr contributing to carbidization sometimes distorts the shape of the graphite incorporation. The complex effect of alloying elements is turning into a strip of white hypoeutectic cast iron – the third zone of the transition layer.

The dispersion of the pearlite component of each zone of the transition layer is different. Redistributions of Ni, Cr, and Si are observed only within the limits of the first zone of the transition layer.

The formation of the second and third zones is associated with a change in the carbon concentration of the pig iron of the bundle.

At 3.86–22.64% Ni in the transition layer, adjacent to the cast alloy, the first zone is observed, in which, at high cooling rates, there are areas of bainite and residual austenite, as well as partially dissolved powder particles CrNi80SiB3. In the second zone, along the grain boundary, carbides from doped cementite of the type $(Fe, Cr)_7C_3$ and cementite needles with a type-magnet orientation are observed clearly. The effect on the structure of the transition layer Cr is significantly manifested at temperatures T_b above the boiling liquid. At the same time, the first zone acquires a troost – sorbitol structure with a cementite net, which turns into a terostat – martensitic one. Redistributions of C, Ni, and Mn in the transition layer are also confirmed by the change in microparticles.

The research results indicate not only the need to take into account the effect of diffusion on the chemical homogeneity of the microparticles, but also indicate the possibility of controlling the whole complex of structural and special properties of powder materials by regulating the processes occurring in the near contact zone.

3. Conclusion. In a cast iron casting, the formation of the structure and properties of a composition coat depends not only on the chemical and fractional composition of the powder particles, but also on the temperature condition of the impregnation of the powder spread with liquid metal.

References:

1. Novruzov G. D., Rasulov F. R. Interaction of liquid iron with a plaster of composites in a centrifugal form – AzTU, Educational, methodical and scientific-technical conference of professors and graduate students, part II- 2001.– P. 247–249.
2. Averbach B. L., Warren B. E. Interpretation of the X-ray Pattens of Coldd-Workrd Metal J. Appl. Plys. 1949.–V. 20.– P. 885–889.
3. Campbell J. Feding Mechanisms in Casting // AFS Cast Metals Researeh Journal. 1989.– V. 5. – No. 1. – P. 20–26.
4. Rasulov F. R. İmproving the properties of the surface of the cast iron by absorbing into the liquid metal in the casting mold. Austrian Journal of Technical and Natural Sciences, Austrian, – Vol. 1. – No. 11–12. 2018. – P. 36–41.
5. Rasulov F. R. Formation of composite coating in casting by impregnation of the powder composite with liquid metal in the process of casting // AzTU Uchenye zapiski, 2010.– No. 2.– Vol. IX (34).– P. 62–66.

Timoshkin Andrey Ivanovich,
Candidate of Physical and Mathematical Sciences, professor
National Metallurgical Academy of Ukraine
E-mail: 33-timoshkin1964@gmail.com

CONDITIONS FOR2-TESTABILITY OF TREE-LIKE CIRCUITS OF SINGLE-OUTPUT FUNCTIONAL ELEMENTS FOR SINGLE STUCK-AT FAULTS ON SIGNAL LINES

Abstract. Elaboration of new efficient mathematical models of testable digital circuits is impossible without determination conditions of existence fault detection tests of definite length, including minimally possible length for circuits of functional elements in respect of stuck-at faults on their signal lines. The necessary and sufficient condition for 2-testability of tree-like circuits of one-bit output functional elements in respect of single stuck-at faults on their signal lines have been obtained.

Keywords: tree-like functional-logical circuits, stuck-at fault, fault detection test.

1. Introduction and research objective

It is impossible to build effective mathematical models of testable digital circuits without providing conditions for tests of a given sequence length, including the minimum possible length, for functional elements circuits for stuck-at faults on their signal lines (i.e., on lines connecting functional elements with each other in logical circuits, as well as at the inputs and outputs of these circuits [1; 2]).

It is obvious, that functional elements circuits may differ in structure. A number of works [1; 3; 4] consider tree-like and iterative block structures most promising in terms of testability. Therefore, the task of determination of conditions for fault detection tests of length 2 existence for different types of tree-like (or irritation-free [1; 3; 5]) circuits for different stuck-at faults is relevant and can be set as following:

The fault class J on signal lines of functional elements is set and tree-like functional elements circuit class E is set. The task is to find necessary and sufficient conditions for existence of fault detection test of length 2 for any tree-like circuits of E class for faults of class J.

This article is devoted to solution of the given task for E_1 subclass of tree-like circuits of single-output functional elements and J class single stuck-at faults.

2. Main results

Let us assume that Σ is a set of logical circuits, each of which contains at least one functional element and does not contain discrete converters with memory [1; 6]. Let us denote a set of signal lines of circuit $S \in \Sigma$ as $A = \{a_1, a_2, ..., a_p\}$ that fulfills at least one of the following conditions for any signal line $a \in A$:

a connects the external poles of the circuit S (2.1)

a connects the functional elements of the circuit S (2.2)

a connects all elements of a certain subset of $I = \Phi \cup V$ (where Φ is the set of all functional elements of the circuit S, V is the set of all external poles of the circuit S), for which both inequalities are true:

$$I' \subseteq I : I' \cap \Phi \neq \varnothing \text{ and } I' \cap V \neq \varnothing \quad (2.3)$$

As can be seen, the following equality is true for any logical circuit:

$$V = X \cup Y \quad (2.4)$$

where X is the set of all input poles (or inputs) of the circuit S, Y is the set of all output poles (or outputs) of the circuit S.

The signal line $a \in \Delta$ of the circuit S (where Δ is the set of all signal lines of the circuit S), connected to at least one input of the circuit S, will be

referred to as the input signal line of the circuit S. The signal line $a \in \Delta$ of the circuit S, connected to at least one output of the circuit S, will be referred to as the output signal line of the circuit S.

It is also obvious that for any logical circuit S the following inclusion is true:

$$A \subseteq \Delta \qquad (2.5)$$

Let us consider subset Σ_1 of set Σ that fulfills the following condition for any circuit $S \in \Sigma_1$:

$$\Delta \subseteq A \qquad (2.6)$$

Let us denote subset of Σ_1 by Σ_2 that is not null for any circuit $S \in \Sigma_2$ of set $A(S)$:

$$A(S) \neq \varnothing \qquad (2.7)$$

Let us denote subset of Σ_2 by Σ_3, such that any circuit $S \in \Sigma_3$ contains functional elements with one-sided (directed) [1] and only with one-sided conductivity.

Any circuit $S \in \Sigma_3$ creates a binary relation ϕ on the set A with the graph $gr\phi \subseteq A \times A = A^2$ [7], defined as follows: the signal lines a_i and a_l of the set A of circuit S are in relation ϕ (i.e. $a_i \phi a_l$) if and only if the signal line a_i connected to the input of a functional element F of the circuit S, and signal a_l to its output.

Let us denote by Σ_4 subset of Σ_3 such that for any circuit $S \in \Sigma_4$ the following is true:

$$gr\phi \neq \varnothing \qquad (2.8)$$

(i.e. the relation ϕ, set by circuit S on the set A is not null). Let us consider collective Θ of m – relations [7] (where $2 \le m \le \infty$) on the set A of the circuit $S \in \Sigma_4$ such that for an arbitrary relationship $\theta^m \in \Theta$ with graph $gr\theta^m \subseteq A^m$ vector (tuple) $\tilde{a}_j = (a_j^{(1)},...,a_j^{(k)},a_j^{(k+1)},...,a_j^{(m)}) \in gr\theta^m$ if and only if the following condition is satisfied:

$$(\forall k \in \{1,2,...,m-1\})(a_j^{(k)} \phi\ a_j^{(k+1)}) \qquad (2.9)$$

(i.e. $(\forall k \in \{1,2,...,m-1\})((a_j^{(k)}\ a_j^{(k+1)}) \in gr\phi)$). This set describes the structure of the system A of signal lines of the circuit $S \in \Sigma_4$.

Let us denote by Σ_5 subset of Σ_4 such that for any circuit $S \in \Sigma_5$ the following is true:

Collective $\Theta(S)$, corresponding to the circuit S, is such that for any vector (tuple) $\tilde{a}_j = (a_j^{(1)},...,a_j^{(k)},...,a_j^{(m)})$, situated on the graph of an arbitrary relation θ^m of Θ, fulfillment of the inequality $s \neq r$ leads to fulfillment of the inequality $a_j^{(s)} \neq a_j^{(r)}$ for any s and r of the set $\{1,...,m\}$ (i.e. the different components of any vector of the graph of any relation θ^m, belonging to $\Theta(S)$, corresponded by different elements of A). (2.10)

The signal line $a_i \in A$, connected to output of element F of the circuit $S \in \Sigma_5$ will be referred to as the output line of the element F. The signal line $a_j \in A$, connected to input of element $F \in \Phi$ of the circuit $S \in \Sigma_5$ will be referred to as the input line of the element F. Inputs and outputs of all functional elements of the circuit $S \in \Sigma_5$, as well as all inputs and outputs of this circuit will be referred to as the circuit contacts S, while inputs and outputs of the element F of the circuit S will be accordingly referred to as the input and output contacts of the element F of the circuit S, inputs of the circuit S will be referred to as the input contacts of the circuit S, and the outputs – as the output contacts of the circuit S.

Let us denote by C the set of all contacts of the circuit $S \in \Sigma_5$. Let us consider a connected geometric figure, formed by all contacts of set $\tilde{C}$ by the elements of some subset $\tilde{A} \neq \varnothing$ of set A of this circuit, as a set of connected $\tilde{C} \subseteq C \left| \left| \tilde{C} \right| > 1 \right.$ contacts of the circuit S. Connection of set $\tilde{C}(S)$ of contacts of the circuit S will be denoted by $\omega(\tilde{C}(S),\tilde{A}(S))$. If contact c_i of the circuit S is contained in set $\tilde{C}$ of contacts of connections $\omega(\tilde{C}(S),\tilde{A}(S))$ of the circuit S, then it shall be considered as a part of connection $\omega(\tilde{C}(S),\tilde{A}(S))$. Let us consider contacts c_i and c_j connected, if and only if c_i and c_j are a part of the same connection in the circuit S (i.e. if and only if contacts c_i and c_j are contained in set of the contacts of some connection ω of the circuit S).

Let us refer to connection $\omega(\tilde{C}(S),\tilde{A}(S))$ of the circuit S as an elementary connection, if it satisfies the following condition $\left|\tilde{A}(S)\right| = 1$ (i.e. in which the contacts are connected by its only signal line). The simplest is the elementary connection $\omega(\tilde{C}(S),\tilde{A}(S))$ of the circuit S, which fulfills the condition: $\left|\tilde{C}\right| = 2$

(i.e. the elementary connection formed from the two contacts of the circuit S). Let us consider contact c_i of the circuit S involved, if and only if the circuit S has a connection $\omega(\tilde{C}(S), \tilde{A}(S))$, in which it is involved.

Let us denote by Σ_6 as a subset of Σ_5 such, that any circuit $S \in \Sigma_6$ contains single-output functional elements, while any single-output functional element F of the circuit $S \in \Sigma_6$ has significant and only significant inputs (i.e. F performs a Boolean function $f \in P_2$, that essentially depends on all its arguments (variables)).

Let us analyze subset Σ_7 of set Σ_6 which fulfills the following conditions for any $S \in \Sigma_7$ circuit:

Any contact c_i of the circuit S is involved. (2.11)

The circuit S contains only the simplest connections of contacts. (2.12)

Any input $x \in X$ of the circuit S is connected to either the output $y \in Y$ of the circuit S, or the input of the element $F \in \Phi$ of the circuit S. (2.13)

Any output $y \in Y$ of the circuit S is connected either to the input $x \in X$ of the circuit S, or to the output of the element $F \in \Phi$ of the circuit S. (2.14)

Any input i_e of any element $F_u \in \Phi$ of the circuit is connected either to the input $x \in X$ of the circuit S, or to the element output $F_v \in \Phi$ of the circuit S. (2.15)

The output of any element $F_g \in \Phi$ of the circuit S is connected either to the output $y \in Y$ of the circuit S, or to the input i_s of the element $F_q \in \Phi$ of the circuit S. (2.16)

$|Y| = 1$ for the circuit S (i.e. the circuit S has a single output). (2.17)

It is easily seen that any circuit $S \in \Sigma_7$ defines one-to-one mapping H of the set $A(S) \setminus A_w(S)$ (where $A_w(S)$ is the set of all input signal lines of the circuit S) on the set $\Phi(S)$. This mapping is defined as follows:

for $\forall a \in A(S) \setminus A_w(S)$ $H(a) = F$ when the signal line a is connected to the output of the element $F \in \Phi$ of the circuit S.

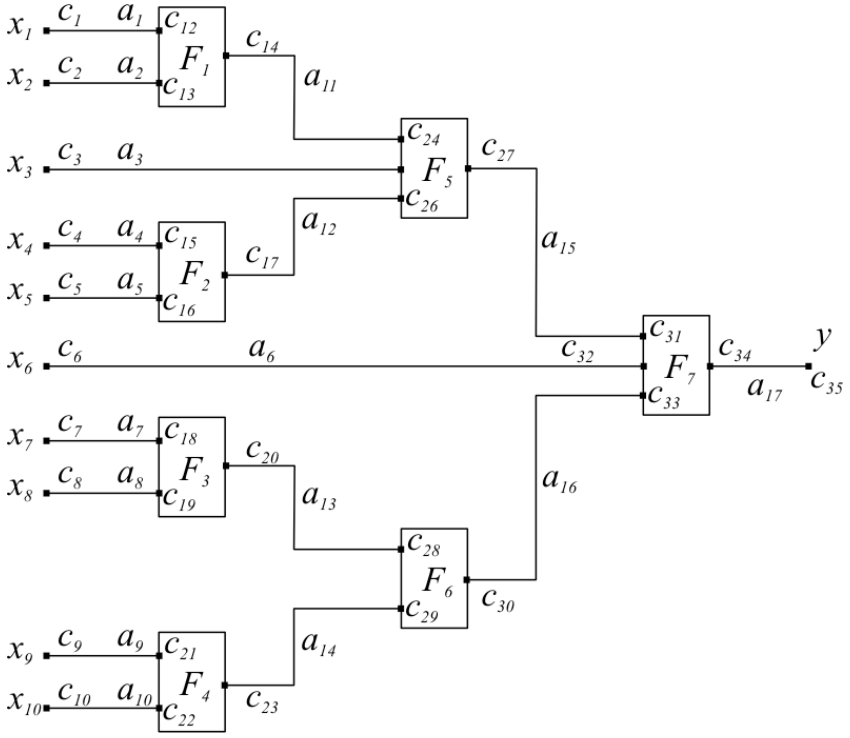

Figure 1. Circuit S_1

It is also easily seen that relation ϕ for any circuit $S \in \Sigma_7$ is functional [7]. The definition domain [8] $D(\phi)$ of the relation in this case is the set $A \setminus \{a_{ou}\}$ (where a_{ou} is the output signal line of the circuit S)

and the range of values $Z(\phi)$ is the srt $A(S)\setminus A_w(S)$ (where $A_w(S)$ is the set of input signal lines of the circuit S). For the output signal line a_{ou} of the circuit $S\in\Sigma_7$ and any signal line $a\neq a_{ou}$ of this circuit exists a single tuple (vector) $\tilde{a}_j=(a_j^{(1)},...,a_j^{(k)},a_j^{(k+1)},...,...,a_j^{(m)})(2\le m<\infty)$ that is $a_j^{(1)}=a,a_j^{(m)}=a_{ou}$ and for $\forall k\in\{1,2,...,m-1\}\quad((a_j^{(k)}\in A)\&(a_j^{(k)}\phi a_j^{(k+1)}))$. This tuple belongs to the graph of some m-relation θ^m of the collective $\Theta(S)$ of m – relations that correspond to this circuit.

Let us assign each signal line $a\in A$ of the circuit $S\in\Sigma_7$ an appropriate level, defined by the following:

1) assign a level 0 to the output signal line a_{ou} of the circuit $S\in\Sigma_7$;

2) assign level $j+1$ to the input lines to the element $F\in\Phi$ of the circuit $S\in\Sigma_7$, where j level of the output line of the element F.

It is obvious, that

$A=\bigcup_{j=0}^{r-1}A_j$ and $(\forall p,q\in\{0,1,2,...,r-1\})\ (A_p\cap A_q=\varnothing)$, where A_j is the set of signal lines of j level and r is the number of levels of the circuit S.

An example of a circuit from a set Σ_7 can be the circuit S_1 shown in (Figure 1).

Any stuck-at fault β of any signal line $a\in A$ of the circuit $S\in\Sigma_7$ can be considered as clamping of signal line on logical 0 or 1.

The necessary and sufficient condition for 2-testability of the circuit S consisting of Σ_7 relatively single stuck-at faults on its signal lines is given by the following theorem:

Theorem 1. A circuit S consisting of Σ_7 has a fault detection test of length 2 for single stuck-at faults on signal lines if and only if

$$(\forall F\in\Phi)(f(F)\in G) \qquad (2.18)$$

where f is the function performed by F, G is the class of Boolean functions performed by 2-testable for single stuck-at faults with single-output functional elements [9].

Reasoning. It is obvious, that condition (2.18) is necessary. Let us prove that this condition is sufficient. Let us construct a vector $b=(\beta_{i_1j_1},...,\beta_{i_uj_u})$ of logical signals values (β_{ij} is the value of a logical signal on i line of j level, $u=|A_w|$) on the input lines of the circuit $S\in\Sigma_7$ using the following algorithm:

Given data: it is assumed that for $\forall j\in\{0,1,...,r\}$ set A_j of signal lines of j level of the circuit $S\in\Sigma_7$ is in a certain order. It is also assumed that for each Boolean function f implemented by at least one functional element from $\Phi=\{F_1,F_2,...,F_z\}$ the circuit $S\in\Sigma_7$, the set $\Psi(f)$ of all pairs of $\tau 2$ – vectors is found (pair of $\tau 2$-vectors of the Boolean function $f(x_1,...,x_n)$ is a pair of binary vectors $b_1=(\beta_1^1,...,\beta_n^1)$ and $b_2=(\beta_1^2,...,\beta_n^2)$, that detect any single replacements of any input and output variables with the constants 0 and 1) [9].

Algorithm 1. *1st step.* It is considered that $j=0$, $A_0=\{a_{ou}\}=\{a_{10}\},\beta_{10}=\beta'\in\{0,1\},B^\Sigma=\varnothing$. *2nd step.* The condition $A_j\cap A_w\neq\varnothing$ is checked. If the condition is met, then the transition to the 3rd step is made. If the condition is not met, then the transition to the 5th step is made. *3rd step.* Set $B_j=\{\beta_{ij}\setminus a_{ij}\in A_j\cap A_w\}$ is formed. *4th step.* $B^\Sigma:=B^\Sigma\cup B_j$. *5th set.* Set $A_j'=A_j\setminus(A_j\cap A_w)$ is formed. *6th step.* The condition $A_j'=\varnothing$ is check. If the condition is met, then $B=B^\Sigma$ and the algorithm is over. If the condition is not met, then the transition to the 7th step is made. *7th step.* For each signal line $a_{ij}\in A_j'$ an corresponding element $F\in\Phi:H(a_{ij})=F$ is determined and for Boolean function f performed by the element, a vector b_l is chosen from any pair of $\tau 2$-vectors of the set $\Psi(f)$, that $f(b_l)=\beta_{ij}$ (where β_{ij} s the logical signal value assigned to the line a_{ij}). The input lines of the element F are assigned the values of the corresponding components of the vector b_l. *8th step.* $j:=j+1$ and the transition to the 2nd step is made.

It is easily seen that the vector constructed using algorithm 1 $b=(\beta_1,\beta_2,...,\beta_n)$ and the vector $\bar{b}=(\bar{\beta}_1,\bar{\beta}_2,...,\bar{\beta}_n)$ opposite to it form a fault detection test of length 2 for the considered circuit for single stuck-at faults on its signal lines. For example, let there are a stuck-at fault $\beta\in\{0,1\}$ on any signal line $a\in A\setminus\{a_{ou}\}$ of the circuit S. With the succes-

sive supply of vectors b and $\bar{b}$ to inputs of the circuit S to inputs of any functional element F of this circuit, the pair of supplied vectors form a fault detection test for single stuck-at faults at its inputs and outputs. Consequently, stuck-at fault β changes logical signal value on the line a, when a vector b or vector $\bar{b}$ is set at the circuit S inputs. Additionally, when any vector of the set $\{b, \bar{b}\}$ is at the inputs of the considered circuit *S* the change in the value of the logical signal on the 1st component of any tuple $\tilde{a}_j = (a_j^{(1)},...,a_j^{(k)},a_j^{(k+1)},...,a_j^{(m)})$ from the any graph of -relation $\theta^m \in \Theta(S)$ causes a change in the value of a logical signal on *m*-component. Consequently, when any vector of the set $\{b, \bar{b}\}$ is at the inputs of the considered circuit *S*, the change in the value of the logical signal on the 1st component of any tuple $\tilde{a}_l = (a_l^{(1)},...,a_l^{(k)},...,a_l^{(s)})$, where $a_l^{(1)} = a, a_l^{(s)} = a_{ou}$ causes a change in the value of the logic signal on its *s* component, i.e. on the output signal line a_{ou} and therefore on the output *y* of the circuit *S*. Thereby, stuck-at fault β on the signal line *a* is detected by input vector *b* or by input vector $\bar{b}$. The sufficiency of condition (2.18) is proved.

3. Conclusion.

The obtained results can be used to develop a number of mathematical models of testable circuits. Subsequent researches will be devoted to creation of necessary and sufficient conditions for 2-testability of tree-like circuits of functional elements for stuck-at faults of the fault class of multiplicity 1 and higher.

Referenses:

1. Казначеев В. И. Диагностика неисправностей цифровых автоматов.– М.: «Советское радио», 1975.– 256 с.
2. Киносита К., Асада К., Карацу О. Логическое проектирование СБИС: Пер. с япон.– М.: Мир, 1988.– 309 с.
3. Кондратьев В. В., Махалин Б. Н. Автоматизация контроля цифровых функциональных модулей.– М.: Радио и связь, 1990.– 152 с.
4. Friedman A. D. Easily testable iterative systems // IEEE Trans. on computers, 1973. – V. 22. – No. 12. – P. 1061–1064.
5. Трахтенброт Б. А. К теории бесповторных контактных схем.– В кн: Труды МИАН СССР. Т. 51.– М.: Изд-во АН СССР, 1958.– С. 226–269.
6. Яблонский С. В. Введение в дискретную математику.– М.: Наука, 1986.– 384 с.
7. Глушков В. М., Цейтлин Г. Е., Ющенко Е. Л. Алгебра. Языки. Программирование.– К.: Наук. думка, 1978.– 320 с.
8. Кук Д., Бейз Г. Компьютерная математика: Пер. с англ.– М.: Наука, 1990.– 384 с.
9. Тимошкин А. И. Об одном классе функций из P_2 // Кибернетика и системный анализ, 2001. – № 5. С. 24–30.

Tyapin Alexey Andreevich,
Postgraduate student, Siberian Federal University
E-mail: Mishinskaya_AS@tamerlan-krk.ru
Kinev Evgeny Sergeevich,
Candidate of technical sciences,
Director Thermal Electric Systems LLC
E-mail: kinev_es@ontecom.com

FOUR-ZONE LINEAR INDUCTION MACHINE WITH TWO-PHASE POWER

Abstract. Linear induction MHD machines with a low-frequency power supply inverter form a complex of electromagnetic stirring of liquid aluminum in melting furnaces. The article discusses the classification features and characteristics of four-zone inductors of a longitudinal magnetic field with a two-phase power supply. To calculate the operating parameters of a linear induction MHD machine, a nonlinear multiphase model of a magnetic circuit was used. As a result of an iterative calculation, the distribution of the integral magnetic fluxes in the tooth zone of a flat inductor is obtained, and vector diagrams of electromagnetic regime parameters are constructed. The study shows the main directions of optimization of the low-pole induction machine mode to obtain the best current distribution in the windings and to estimate the equivalent linear current load. According to the results of the analysis, the main tasks and the sequence of stages of their solution were formulated when developing energy-efficient induction MHD machines of a longitudinal magnetic field.

Keywords. Induction MHD machine, inductor of longitudinal magnetic field, electromagnetic stirrer, running magnetic field, multiphase magnetic circuit model, vector magnetic flux diagram, two-phase power supply system, frequency inverter.

For stirring metal melts in furnaces, linear induction machines of transverse and longitudinal magnetic fields are used [1, p. 2]. The cost of each technical solution, along with the technological and energy efficiency of induction machines and power sources, is a decisive factor in the decision to modernize production or to develop design solutions for new construction of smelting furnaces [2, p. 217]. As induction machines for stirring aluminum alloys in mixers and furnaces, in addition to transverse field inductors, high-tech shortened inductors of the longitudinal field are used [3, p. 65]. Among the simplest flat induction MDG machines, two constructive solutions can be distinguished, which determine the type of machine, according to the number of force inducing windings (inducing zones).

These design features appropriately characterize the pole position of the inductor and the magnitude of the synchronous velocity of the runnling magnetic field in the melt [4, p. 26]. The following designations are used as constructive and operational parameters in the description:

2p – is the number of poles of the inductor;

Z – is the number of teeth of the core;

q – is the number of grooves of the core per pole and phase;

a – is the phase zone of the inductor;

m – is the number of phases of a multiphase winding inductor;

Δ – is the working gap.

The classical induction MHD machine of a longitudinal magnetic field can have four or three windings

(a four-zone or three-zone inductor). In addition, the power supply of induction machines can be provided in a two-phase or three-phase version. Thus, when developing inductors and evaluating their effectiveness, four main options should be considered for constructing shortened low-pole induction machines of a longitudinal magnetic field [5, p. 86].

1. Four-zone inductor with two-phase power supply.

$$2p = 2, Z = 5, q = 1, m = 2, \alpha = 90°$$

2. Four-zone inductor with a three-phase power supply.

$$2p = 4/3, Z = 5, q = 1, m = 3, \alpha = 60°$$

3. Three-zone inductor with a two-phase power supply.

$$2p = 3/2, Z = 4, q = 1, m = 2, \alpha = 90°.$$

4. Three-zone inductor with a three-phase power supply.

$$2p = 1, Z = 4, q = 1, m = 3, \alpha = 60°.$$

This article discusses some of the classification characteristics and features of four-zone inductors of a longitudinal magnetic field with two-phase power. A sketch of the construction of a shortened induction MHD machine is shown in (Fig. 1).

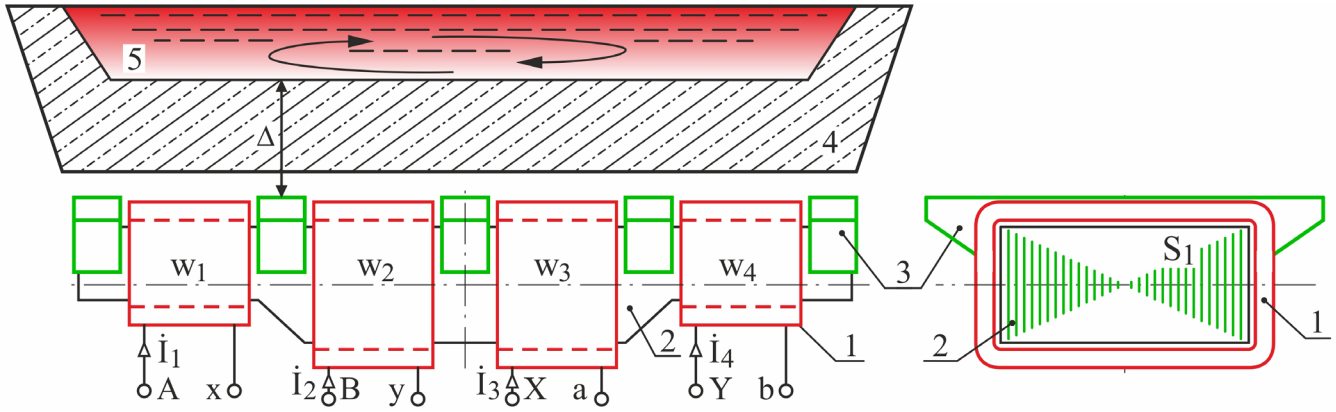

Figure 1.

The inductor has four windings 1, denoted w_1, w_2, w_3, w_4. They are made in the form of two-way disk sections, which are grouped in series or parallel connection. The windings are placed on a steel laminated magnetic core 2, in the middle part of which a thickening is provided, designed to reduce saturation. Between the windings 1 are placed steel teeth 3, which serve as magnetic field concentrators. In the windings connected to the inverter, alternating currents occur at a frequency of about 1 Hz, which create a traveling magnetic field in the surrounding space and capacitance 4 with aluminum melt 5 [6, p. 50].

For this design of the inductor, a two-phase power supply from the transistor inverter of the modified voltage can be applied, and the inductor becomes a four-pole, with a corresponding change in the traction characteristics. By inverting the phases of a pair of windings, they change the polarity of the induction machine (IM). The presence of four windings allows to increase the raster of the coating of the molten metal, located in the region of the dentate zone, by magnetic flux [4; 5].

For presented in fig. 1 letter designation of the A × ByXaYb windings is obtained by a system of balanced voltages in a two-phase configuration with a phase shift of voltages of about $\pi/2$. There is an effect of the mutual influence of currents and distortion of the field pattern due to edge effects and the open-ended configuration of the magnetic circuit, as well as power transfer between the windings due to mutual inductance. Due to the proximity of the windings on the common magnetic core, the phase shifts of currents differ from $\alpha = \pi/2$, therefore the refined distribution of magnetic fluxes is estimated by calculation and experiment, and to control the amplitude-phase relations, measures

of modal regulation, special circuit solutions and algorithmic control of the transistor state inverter [7, p.54].

An example of a spatial phase representation of the mode characteristics for the steady state of an idealized inductor with a power source is shown in (Fig. 2).

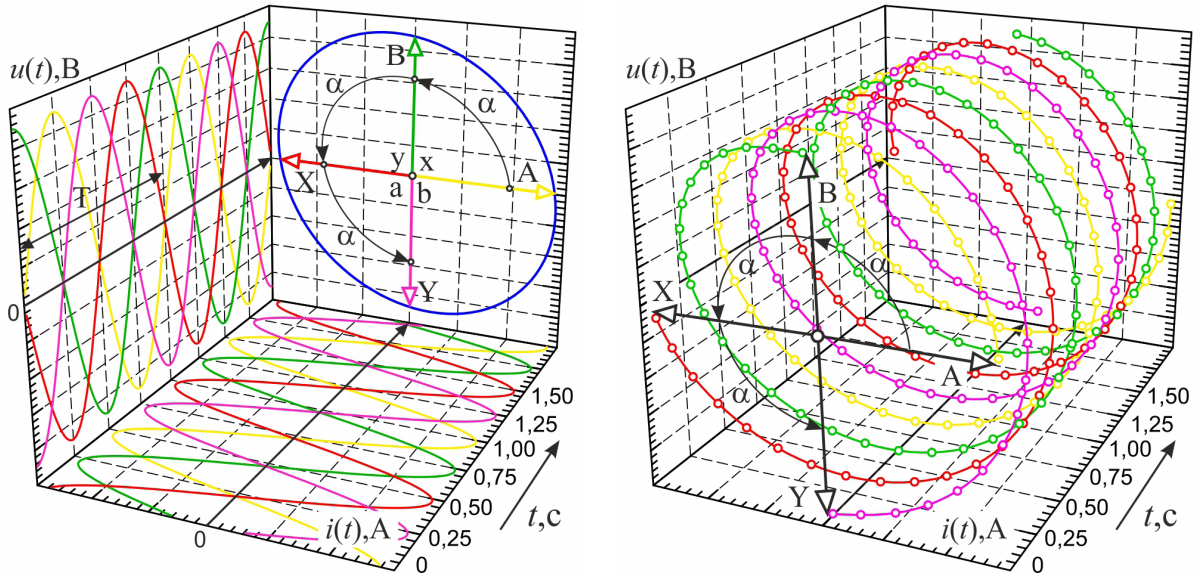

a) b)

Figure 2.

The use of phase coordinates allows us to show vector diagrams of currents, voltages and magnetic fluxes more clearly. The nature of the multi-phase power supply system is largely determined by the wiring diagram of the inducing windings. It should be noted that in the considered two-phase configuration of the MHD inductor, the IM power supply system, in contrast to the three-phase one, is balanced, therefore the side effects caused by the pulsating component of the magnetic field are significantly weakened compared to the use of three-phase power supply. In addition, the power and vibration loads on the metal structures of the inductor and frequency converter, as well as additional losses, are significantly less [3; 5; 8].

A distinctive feature of the power mode of the windings of a two-phase machine can be considered as a separate pair connection of sections to half-bridges of a transistor source. The phasing of the half-bridges of the power link of the inverter is performed in such a way as to ensure a phase shift of about $\pi/2$ between the currents of adjacent windings. An example of the connection scheme of the windings of a two-phase induction machine is shown in fig. 3 In addition to the four-pole variant of the inclusion of the windings of the four-zone inductor, for the presented design of IM, a bipolar inclusion is possible. Changing the number of poles is performed by switching the windings and changing the power supply circuit.

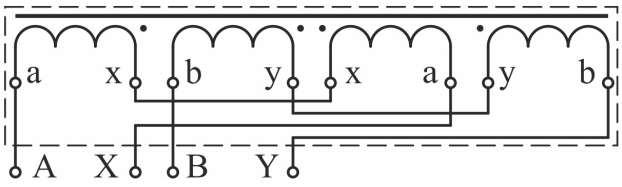

Figure 3.

Changing the polarity certainly leads to a change in the traction characteristics, therefore, for each configuration of a longitudinal magnetic field inductor, the effectiveness of the effect on the melt is estimated in advance and recommendations are made for the use of each type of induction machine [3; 6].

Judging by the scheme, each pair of windings of one phase is connected in series with each other. Such a connection provides the specified distribution of the magnetomotive forces, according to the initial vector diagram, in (fig. 2). It should be noted that the presence of edge effects causes distortion of the field pattern, therefore, the given initial distribution should be considered idealized. If necessary, advanced regulation of the linear current load inductor, the connection diagram of the windings of (fig. 3) can be modified and transferred to the mode of separate connection of phases to the inverter with an increased number of half-bridges, or a parallel connection of windings is realized. However, such decisions are made in advance, since they require additional research and coordination on the current of the inductor mode with the inverter. For parallel connection of the windings, a design solution with a reduced cross-section of the copper bus is required in order to preserve favorable proportions of the inverter utilization ratio by voltage.

An example of the distribution of the integral working flows of the dentate zone in a longitudinal axial section of the inductor is shown in (Fig. 4, a). The distribution diagram for the teeth of the MDS vectors of the balanced system of currents in the reverse order of the phase rotation is shown in (Fig. 4, b).

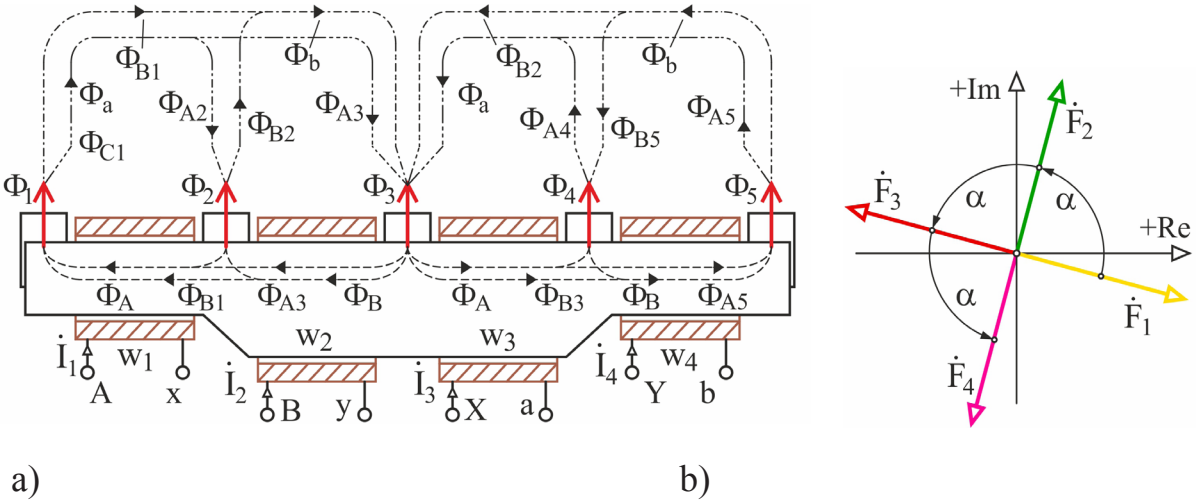

a) b)

Figure 4.

The calculation of the electromagnetic mode of the induction machine of the longitudinal magnetic field is conveniently performed using a multiphase model of a magnetic circuit [4; 9]. The structure and parameters of the model are determined by the actual geometry of the inductor and the winding mode. The specified magnetizing effects take the values of equivalent sinusoid currents, taking into account saturation for a given inductor mode. According to the results of the parametric optimization of the distribution of integral fluxes of teeth, increased values of the magnetizing forces of the extreme windings can be applied, according to the condition of the greatest achievable uniformity in a circular raster [9; 10]. Optimization criteria may be different, more complex, directly taking into account the developed tractive effort in the molten aluminum.

A fragment of the spatial circuit model of a two-phase nonlinear magnetic circuit is shown in (Fig. 5). The construction and determination of the parameters of a detailed magnetic circuit model is considered in [9; 10]. A feature of the presented model can be considered the use as magnetizing sources, controlled four-pole links. The principle of analogy of electrical

and magnetic circuits [4; 10] is used. The matrix description of the controlled source of magnetic voltage corresponds to the traditional four-pole element of the theory of circuits, referred to as a voltage source controlled by current. The magnetization control mode allows changing the coefficients k_1, k_2, k_3, k_4 to take into account the changing harmonic composition when magnetizing the steel magnetic circuit. It should be understood that, by the principle of a formal analogy of electric and magnetic circuits, we are talking about sources of magnetic voltage (magnetomotive force), controlled by magnetic flux or magnetic voltage.

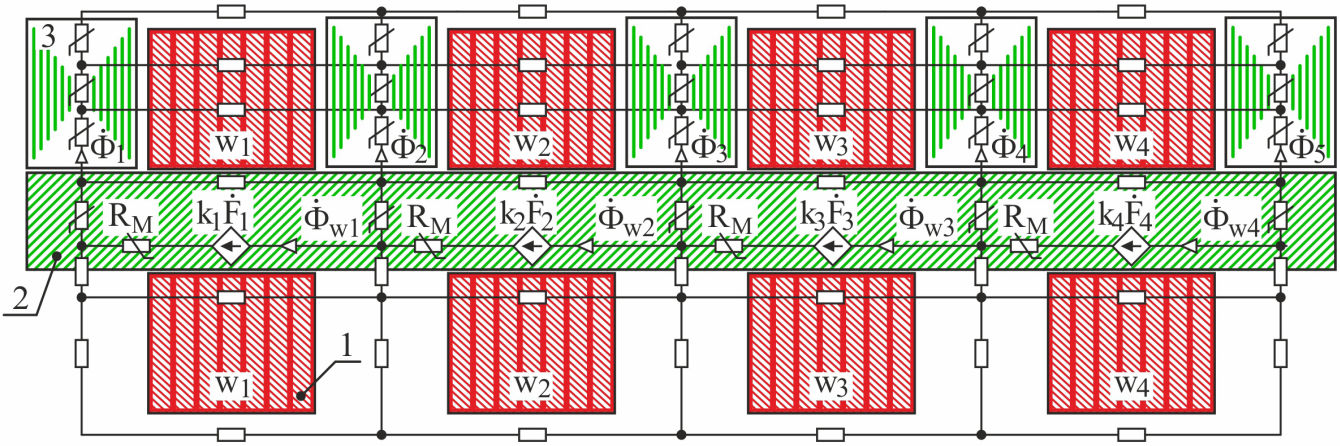

Figure 5.

The solution of the nonlinear problem is performed by the methods of the theory of chains, using a modified nodal analysis. Therefore, a matrix image corresponds to each element of the circuit model, and a system of equations of 5–6 orders of magnitude is formed for each controlled source, and a second order for passive elements in the conducive format. When using n-sensors of magnetic flux in the circuit structure, the dimension of the system increases proportionally by 2n. It can be noted that the final dimension of a nonlinear iterative problem is not decisive, since modern computing resources have overcome possible limitations [11; 12]. Practical iterative calculations showed that in the steady state in the center of the magnetic circuit, the relative magnetic permeability can be reduced to 20–30 units with a corresponding increase in the magnetic resistance (H^{-1}) of the chain section. The order of complexity of the model can be quite significant, but the study showed that an increase in the number of nodes, for example from 200 to 1000, with correct determination of the integral parameters of the chain model, does not lead to a significant increase in the accuracy of the calculation [12, p. 208].

The description of the mathematical model is formed manually, in a text format in ASCII code, similar to some versions of the Ansys software package. Repeat fragments can be declared models and grouped in a compact form.

The results of an iterative calculation of the electromagnetic mode of IM are presented in the form of a vector diagram. The distribution diagram for the teeth of the amplitude vectors of the working magnetic fluxes is shown in (Fig. 6). The diagram shows the expanded raster of the magnetic field vectors above $7 \neq / 6$, with a circular movement counterclockwise from the Φ1 vector to the Φ5 vector. This suggests that the raster leaves the magnetic poles of the four-zone inductor with a two-phase power supply beyond the full circle for the case of $2p = 2$.

Regulation of the magnetizing force of the windings carry out the redistribution of tooth flows, changing their intensity and phase shifts. Naturally, with a pair of head-on switching windings of differ-

ent phases, the possibilities of regulation are limited, even if there is software and algorithmic control of the inverter mode.

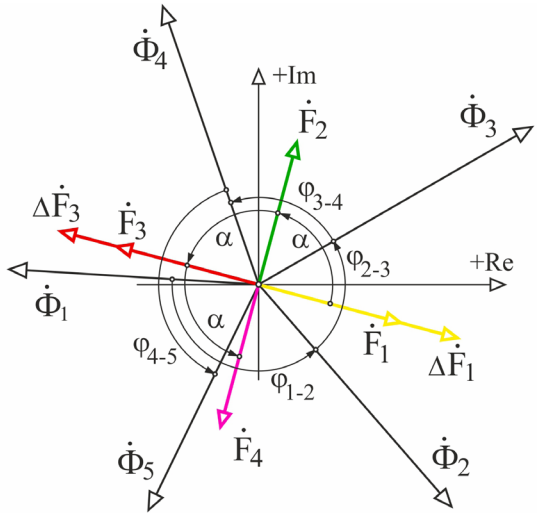

Figure 6

It should be noted that a detailed study of the possibility of controlling the shifts of magnetic fluxes is the subject of parametric optimization. In this case, the optimization criteria can be set significantly different, both for uniform distribution of the prong flows, and for extremely non-uniform. An additional parameter in the design of the optimization target function is the tractive effort in the melt developed by these flows [12–14]. It is noteworthy that it is in the two-phase power supply system that there are expanded possibilities for separate control of the windings of the induction machine, while the three-phase system is limited in control capabilities, since it is coherent.

It should be noted that the results presented here should be considered as a statement of the problem and a first approximation to the calculation of the electromagnetic mode in the development format of an induction MHD machine of the above configuration.

Conclusion. When building energy-efficient induction MHD machines, several interrelated problems should be solved. Evaluation of the effectiveness of the effect of inductors on the molten metal when changing the operating characteristics is the essence of the magnetohydrodynamic problem. The study of the characteristics and features of the electromagnetic field of an induction machine, as well as the methods of controlling the redistribution of magnetic flux, relates to the field of mathematical modeling and optimization of the inductor magnetic system. Creating an effective winding switching circuit, controlling the number of poles and the speed of a traveling magnetic field should also be considered as a task in the field of research into flat induction machines of a longitudinal magnetic field. In addition, it should be understood that the standard three-phase inverters of a rotating asynchronous electric drive are unsuitable for powering metallurgical equipment, the modes of which are sharply asymmetric and extreme. Therefore, when constructing complexes of various dimensions intended for electromagnetic mixing of the melt, it is necessary to create a series of economical and reliable power sources for induction machines, with a different number of phases and various circuitry for switching windings. Each of the indicated tasks for the whole variety of designs of induction machines is rather complicated and it is necessary to devote a separate study to it.

References:

1. US Patent, № 9901978B2. Metod and aparatus for moving molten metal. Pavlov Evgeny, Ivanov Dmitry, Gassanov Pavel, Gulayev Andrew. – Feb. 27, 2018.
2. Krumin' Yu. K. Osnovy teorii i rascheta ustroystv s begushchim magnitnym polem [Bases of the theory and calculation of devices with the running magnetic field]. Riga. Zinatne Publishing House, 1983. – 278 p.
3. Tyapin A. A. Inductors for electromagnetic stirrers // Znanstvena Misel Journal. 2018. – No. 19. – Vol. 1. – P. 64–67.

4. Kinev E. S., Tyapin A. A., Golovenko E. A., Avdulova Yu. S. [Management of casting of aluminum from the stationary furnace]. The Omsk scientific bulletin. 2019. – No. 1 (163). – P. 26–33. DOI: 10.25206/1813-8225-2019-163-26-33. (in Russ.)
5. Golovenko E. A., Goremykin V. A. [Technology of electromagnetic impact on aluminum fusion in mixers and furnaces]. Tsvetnye metally. [Non-ferrous metals], 2014. – No. 2 (854). – P. 86–92. (in Russ.)
6. Tyapin A. A. The structure of electromagnetic stirrers // Znanstvena Misel Journal. 2018. – No. 20. – Vol. 1. – P. 50–57.
7. Chaplygin E. E. Vilkov A. E., Hukhtikov S. V. [Pulse-width modulation with a passive phase in tension inverters with the additional halfbridge]. Electricity. 2012. – No. 8. – P. 53–61. (in Russ.)
8. Tyapin A. A., Andrushchenko V. Yu., Goremykin V. A., Kinev E. S. [Estimation of the penetration depth of an electromagnetic wave into molten aluminum]. Otsenka glubiny proniknoveniya elektromagnitnoy volny v rasplavlennyy alyuminiy. Collection of articles of the XV International Scientific Practical Conference "Innovative scientific research: theory, methodology, practice." Penza: Science and Enlightenment. 2018. – P. 27–34. ISBN978-5-907135-01-7.
9. Sarapulov F. N., Sarapulov S. F., Shymchak P. Matematicheskie modeli lineynykh induktsionnykh mashin na osnove skhem zameshcheniya [Mathematical models of linear induction machines on the basis of equivalent circuits]. – Yekaterinburg: Public Educational Institution of Higher Professional Training UGTU-UPI. 2005. – 431 p.
10. Kinev E. S., Tyapin A. A., Yefimov S. N. [Assessment of the asymmetry of the induction machine with the parameters of symmetrical components] Bulletin of the Voronezh State Technical University. 2018. – T. 14. – No. 6. – P. 68–79. (in Russ.)
11. Morozov E. A. Muyzemnek A. Yu., Shadsky A. S. ANSYS v rukakh inzhenera. [ANSYS in the engineer's hands]. – M.: Lenand Publishing House, 2018. – 456 p.
12. Kinev E. S., Tyapin A. A. [Circuitry connecting IGBT-inverter to a multi-phase induction machine]. Skhemotekhnika podklyucheniya IGBT-invertora k mnogofaznoy induktsionnoy mashine. Collection of scientific papers of the II International Scientific and Practical Conference "CAD and modeling in modern electronics." – Bryansk: BSTU, 2018.– Part 1.– P. 208–215. DOI: 10.30987/conferencearticle_5c19e61d557532.76134464
13. Timofeev V. Application of MHD technology in non-ferrous metallurgy in Siberia / V. Timofeev, M. Khatsayuk, A. Avdulov, G. Lybzikov // 9th International conference on Fundamental and aPlied MHD "Thermo acoustic and Space technologies PAMIR – 14". – Riga. 2014. – P. 101–105.
14. Avdulov A. Electromagnetic Modification of Aluminium Ingots in Rotary Casting Machine / A. Avdulov, I. Gudkov, Y. Avdulova // Applied Mechanics and Materials, Trans Tech Publications, Switzerland. 2015. – Vol. 698. – P. 193–198.

Section 4. Chemistry

Kadirova Shaxnoza Abdukhalilovna,
Doctor of Chemical Sciences, Professor of General and inorganic chemistry Department,
National University of Uzbekistan named after Mirzo Ulugbek

Torambetov Batirbay Smetovich,
PhD student of Department "General and inorganic chemistry" of the faculty of Chemistry,
National University of Uzbekistan named after Mirzo Ulugbek,

Toshmurodov Turdibek Turdimurodovich,
Junior researcher of laboratory "Organic sintesis"
Institute of the Chemistry of Plant Substances,
Academy of Sciences of the Republic of Uzbekistan

Ziyaev Abdukhakim Anvarovich,
Candidate inchemical science, senior researcher of laboratory "Organic sintesis"
Institute of the Chemistry of Plant Substances, Academy of Sciences of the Republic of Uzbekistan

Azimova Durdona Abdullaevna,
Master student of the Department of "General and inorganic chemistry" of Chemical faculty,
National University of Uzbekistan named after Mirzo Ulugbek
E-mail: .....

SYNTHESIS AND INVESTIGATION OF COORDINATION COMPOUNDS OF ZINC AND COPPER NITRATES WITH 2-ETHYLTHIO-5-ACETAMIDO-1, 3, 4-THIADIAZOLE

Abstract. The coordination compounds of salt nitrates Zn(II) and Cu(II) on the basis of ligand 2-ethylthio-5-acetamido-1, 3, 4-thiadiazole were synthesized. The synthesized compounds were investigated using the methods of elemental analysis, IR, ESI-mass spectroscopy and thermal analysis. As results, it was concluded that in the complex the ligand is coordinated to metals through the oxygen atoms of the carbonyl group and the nitrogen of the thiadiazole ring.

Keywords: 3d-metals, zinc, copper, 2-ethylthio-5-acetamido-1, 3, 4-thiadiazole, ligand, IR spectra, ESI-mass spectroscopy, structure, composition, thermal analysis.

A comprehensive study of complexation reactions, the identity of the reaction mechanism, the formation of complex compounds in solution and their isolation in solid form is of undoubted theoretical

and practical interest. In addition, the theoretical and practical results of complex formation reactions with different classes of ligands make it possible to create new complexes, develop new methods for determining metals and obtain highly pure substances, as well as compounds with biologically activity properties.

Derivatives of thiadiazoles are of particular importance among heterocyclic compounds. From the literature [1–4] it is known that thiadiazole derivatives exhibit antibacterial, antimicrobial, herbicidal, and fungicidal properties. Interest in complexes of 3d-metals with biologically active heterocyclic ligands, in particular with thiadiazoles, is primarily due to the prospects of their use as biological preparations in medicine and agriculture [5–7]. The presence of several donor atoms in the thiadiazole molecule contributes to the formation of numerous coordination compounds with transition metal ions with mono- and bidentate coordination of ligands.

As the analysis of literature data shows, despite the fact that the history of the development of the chemistry of heterocyclic compounds has not been for a decade, the field of research of heterocyclic compounds based on thiadiazole derivatives as ligands of coordination compounds is insufficiently studied. Although the search among them is a special type of biologically active substances, given the phenomenon synergism seems to be very promising [7–8].

The purpose of the work is the synthesis and study of the coordination compounds of zinc and copper nitrates with 2-ethylthio-5-acetamido-1, 3, 4-thiadiazole.

The 2-ethylthio-5-acetamido-1, 3, 4-thiadiazole used as the ligand in the complex compounds (L, amorphous powder, with a gross formula $C_6H_9N_3OS_2$, mp. 194–196 °C, is well soluble in alcohols) was synthesized according to the method [9].

The synthesis of zinc nitrate complex with 2-ethylthio-5-acetamido-1, 3, 4-thiadiazole was performed by mixing hot 70% methanol solutions of the metal salt and ligand. The reaction mixture was boiled for 2 hours, filtered, left to crystallize for several days. After a time, small crystalline precipitate fell out, which was filtered, washed with methanol and dried in air. Expected yield of the product, determined T_{melt}. and the nature of the solubility of the compounds obtained.

According to primary studies, it was determined that the complex was obtained in 70% yield, melted at 243 °C, the resulting complex is well soluble in water. According to the results of elemental analysis, it was identified that the following gross formula corresponds to the complex: $ZnC_{12}H_{22}N_8O_{10}$ (Table 1). The complex with copper nitrate was obtained in a similar way.

Table 1. – Yield, melting point and elemental analysis results of zinc (II) and copper (II) complexes based on 2-ethylthio-5-acetamido-1, 3, 4-thiadiazole

Compounds	Yield,%	$T_{melt.}$, °C	Gross-Formula	Found/Calculated,%			
				C	H	N	O
$[ZnL_2(H_2O)_2](NO_3)_2$	70	243	$ZnC_{12}H_{22}N_8O_{10}S_4$	22,2/22,8	3.4/3.5	17.2/17.7	25.4/25.2
$[CuL_2(H_2O)_2](NO_3)_2$	73	225	$CuC_{12}H_{22}N_8O_{10}S_4$	22,8/22,3	3.5/3.7	17.8/17.3	25.4/27.1

Table 2. – The main absorption bands in the IR spectra of the ligand and complexes of zinc and copper nitrates based on it, cm^{-1}

Types of vibrations	ν_sC=O	ν NH δ NH	ν_sC-N ν_{as}C-N	ν_sC=N	ν_s-N=N- ν_{as}-N=N-	ν_{as} CH_2 ν_s CH_2	νM→O νM→N
1	*2*	*3*	*4*	*5*	*6*	*7*	*8*
L	1698	3156 1457	1253 1304	1557	1008 1046	3048 2931	

1	*2*	*3*	*4*	*5*	*6*	*7*	*8*
$[ZnL_2(H_2O)_2](NO_3)_2$	1670	1440	1193 1224	1474	956 1054		550 425
$[CuL_2(H_2O)_2](NO_3)_2$	1622	1486	1293	1486	964 1026		558 430

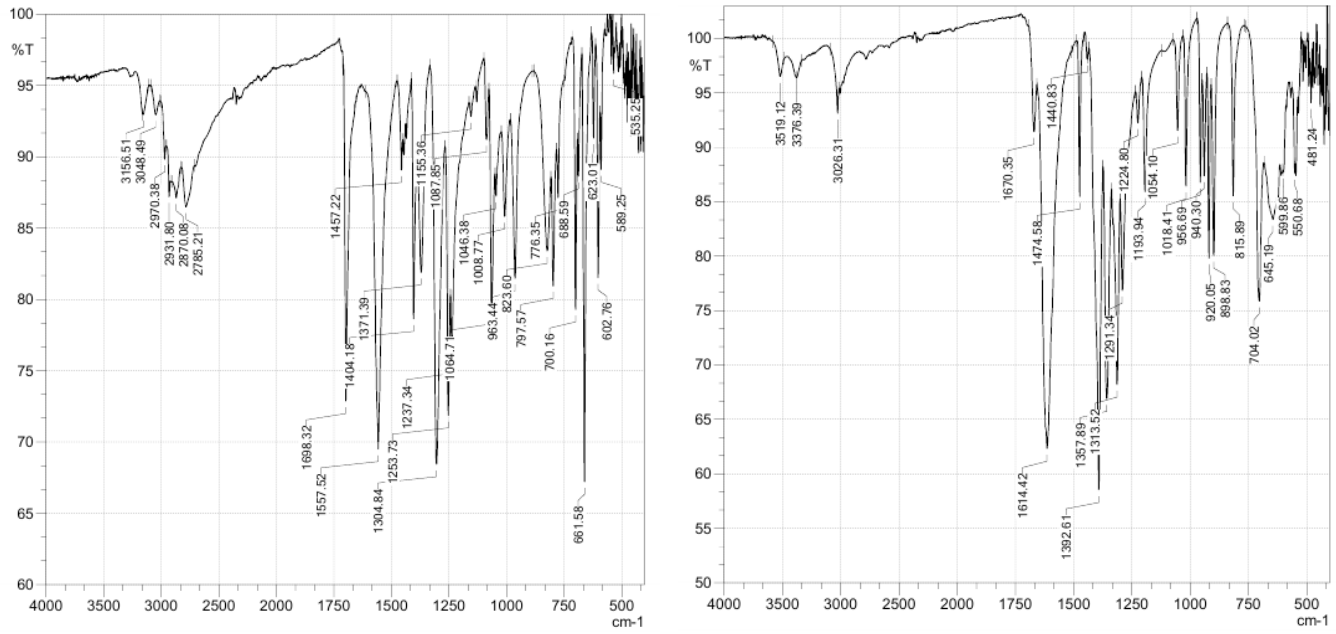

а) б)

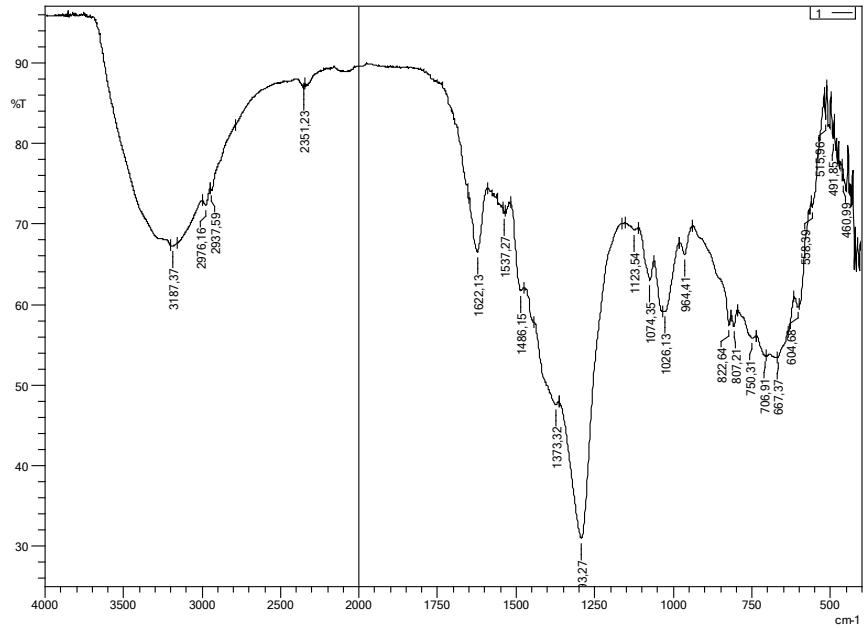

с)

Figure 1. IR spectra of ligand (a) and complexes of Zn (II) nitrate (b) and Cu (II) (c) based on it

To determine the coordination centers in the ligand molecule, an IR spectroscopic study of the complexes was carried out [10].

Interpretation of the IR spectrum of the Zn(II) nitrate complex (Table 2) showed that the absorption bands of symmetric stretching vibrations of the C=O bond undergo significant changes at 1698 cm^{-1} and shift to the low frequency region and manifest themselves at 1670 cm^{-1}. The absorption band of symmetric stretching vibrations of the C=N group from 1557 cm^{-1} to 1474 cm^{-1} also changes, shifting to the low-frequency region by ~ 83 cm^{-1} compared to the position in the IR spectrum of the free ligand. From that it can be deduced that, when coordinating to the complexing ion, two heteroatoms are involved in the ligand molecule – the N^4 atoms of the heterocycle and the oxygen of the carbonyl group of the acetylamine substituent. In the IR spectrum of the complex, in contrast to the spectrum of the free ligand, in the low-frequency region at 550 cm^{-1} and 425 cm^{-1}, new bands appear, attributed, according to [5], to vibrations of the M–O and M–N bonds.

The spectrum of the complex also showed (ν(O–H) 3376 cm^{-1}, deformation vibrations at 1614 cm^{-1}, pendulum vibrations at 704 cm^{-1}) new bands corresponding to the absorption bands of the coordinated water molecule.

To determine the relative molecular mass and quantitative study of the complexes, the samples were analyzed by HPLC-mass spectrometry.

ESI mass spectrometry (electrospray) was used to obtain mass spectra of substances using a 6420 Triple Quad LC / MS mass spectrometer (Agilent Technologies, USA). The mass spectra of the sample was recorded with positive ionization. The intensity of the fragmenter is 10.0 V, the gas flow rate of the desiccant is 12 *l*/min, the gas temperature is 300 °C, the gas pressure on the needle of the sprayer is 20 psi, the evaporator temperature is 300 °C, and the voltage on the capillary is 4000V.

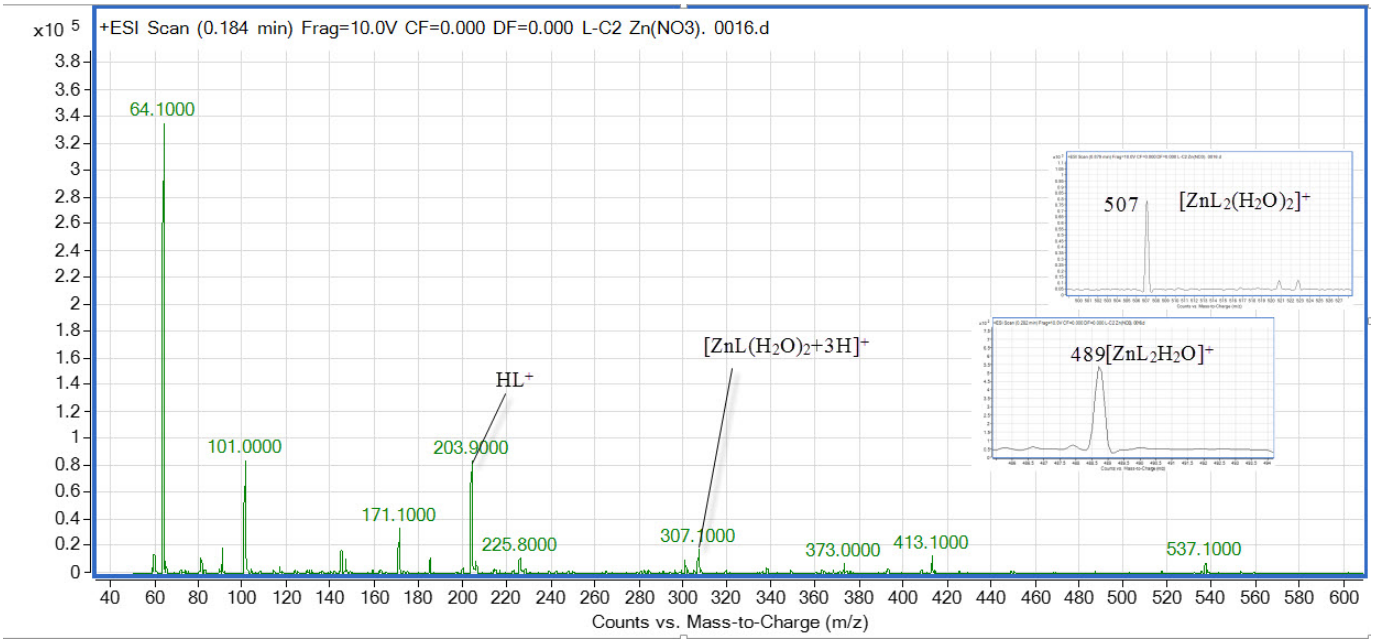

Figure 2. Mass spectrum of the complex of Zn (II) nitrate based on the ligand 2-ethylthio-5-acetamido-1, 3, 4-thiadiazole, taken under the conditions of ionization by spraying in an electric field, the solvent is acetonitrile

In the ESI–MS spectra of the $Zn(NO_3)_2$ and L complex, four types of complex ions are observed: $[ZnL_2NO_3]^+$, $[ZnL_2(H_2O)_2]^+$ $[ZnL_2H_2O]^+$ and $[ZnL(H_2O)_2]^+$ (Fig. 2). In the spectrum there is no sharpness peak of the molecular ion M^{+*}, however, there is a peak with m/z = 537. The most intense in the

spectrum are the peak Zn^{2+} (m/z = 64) and HL^{+} (m/z = = 203.9). As a result of the fragmentation of M^{+*}, peaks appear with m/z = 537.1, m/z = 507, which showed that there are two ligand molecules around the zinc ion — a nitrate anion and water molecules. The nature of ESI–MS fragmentation for the $[ZnL_2(H_2O)_2]^+$ complex (m/z = 507) indicates a loss of $–H_2O$, which corresponds to an unstable ion with m/z = 489 (Fig. 3) with a low intensity. At the next stage, the loss of one ligand molecule from the complex resulted in a more stable ion with m/z = 307. Then we observed a loss of the second ligand molecule, which causes the formation of an ion consisting of two water molecules and zinc with m/z = 101 (Fig. 3).

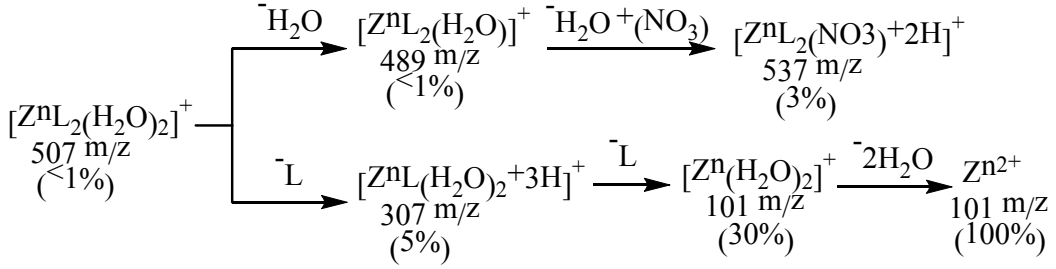

Figure 3. Fragmentation of complex $[ZnL_2(H_2O)_2]^+$

The results of the spectral data obtained for the synthesized complexes show that the studied ligand is coordinated to the central atom by the nitrogen atoms N^4 of the heterocycle and the oxygen of the carbonyl group. According to the results of spectral analysis, it was found that the water molecule is also coordinated in the inner sphere, and the nitrate acidoligand is extra-sphere, and the coordination polyhedron probably has an octahedral configuration.

To determine thermal stability and mass loss with increasing temperature, the method of thermal analysis was applied.

Thermo-analytical studies of the samples were performed on a Netzsch Simultaneous Analyzer STA 409 PG (Germany) instrument, with a K-type thermocouple (Low RG Silver) and aluminum crucibles. All measurements were carried out in an inert nitrogen atmosphere with a nitrogen flow rate of 50 ml/min. The temperature range of measurements was 20–400 °C, the heating rate was 5 K/min. The amount of sample per measurement is 3 mg. The measuring system was calibrated with a standard set of substances KNO_3, In, Bi, Sn, Zn.

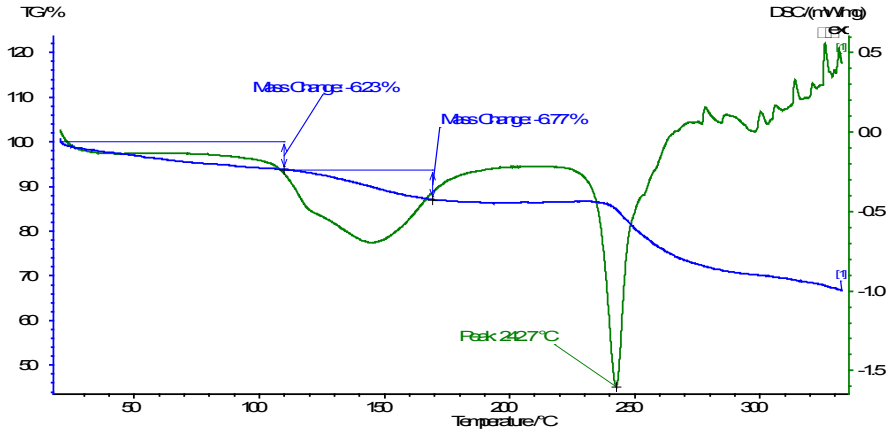

Figure 4. Thermal analysis of the complex $[ZnL_2(H_2O)_2](NO_3)_2$

Thermocatalytic studies were conducted in the temperature range from 20 to 400 °C. In this interval, two areas of weight loss with an endothermic process are observed on the TG curve: the

first is from 110 °C to 170 °C –6.77% (DSC peak T_{max}=144.2 °C, which corresponds to the removal of two water molecules from the internal sphere of the complex, the second section 240–270 °C (DSC peak T_{max}=242.7 °C) corresponds to the melting and decomposition of nitrate anions with the release of NO_2 and O_2. The enthalpy of these two processes is –243.9 and –210.8 J/g/, respectively.

Based on the conducted studies, it can be concluded that the synthesized coordination compounds of zinc and copper nitrates have an octahedral structure, where two molecules of the heterocyclic ligand are coordinated by the bidentate, the fifth and sixth places in the coordination polyhedron are water molecules. According to the results of physico-chemical studies of the synthesized complexes, we can offer the following structure:

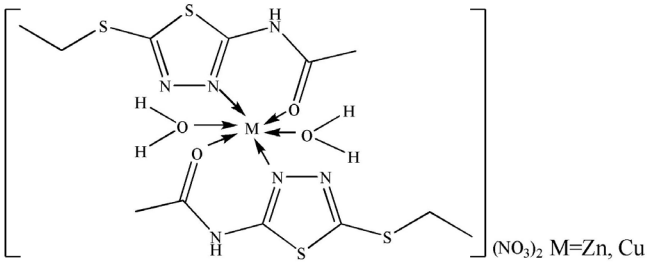

$(NO_3)_2$ M=Zn, Cu

References:

1. Melnikov N. N. Pesticides. Chemistry, technology and application. – M.: Chemistry// 1987. – 612 p.
2. Popiolek L., Biernasiuk A., Malm A. New 5-substituted-1, 3, 4-thiadiazole-2(3H)-thione derivatives: synthesis and there in vitro antimicrobial properties// Amer. Chem. Sci. J., – No. 6.2015. – 136 p.
3. Toshmurodov T. T., Ziyaev A. A., Elmuradov B. Zh., Ismailova D. S., Kurbanova E. R. Highly Selective Synthesis and Fungicidal Activity of the Novel 2-Alkylthio-5-Amino-1, 3, 4-Thiadiazoles// Journal of Chemistry and Chemical Sciences, – Vol. 6(3),2016. – March, – 199 p.
4. Sunduru N., Sharma M. & Chauhan P. M. S. Recent advances in the design and synthesis of heterocycles as antitubercular agents // Future Med. Chem. 2(9),–2010. – 1469 p.
5. Ahmed Y. B., Merzouk H., Harek Y., Medjdoub A., Cherrak S., Larabi L., Narce N. In vitro effects of nickel (II) and copper (II) complexes with 2,5-bis(2-pyridyl)-1, 3, 4-thiadiazole on T lymphocyte proliferation and intracellular redox status// Med Chem Res. 24,2015. – 764 p.
6. Chandra S., Gautam S., Kumar A., Madan M. Coordination mode of pentdentate ligandderivative of 5-amino-1, 3,4-thiadiazole-2-thiol with nickel(II) and copper(II) metal ions: synthesis, spectroscopic-characterization, molecular modeling and fungicidal Study// Spectrochimica Acta Part A: Molecular and Biomolecular Spectroscopy.2014.
7. Mahasin Alias, Huda Kassum, Carolin Shakir. Synthesis, spectral, thermal and antibacterial studies of Cd(II), Mn(II) and Fe(III) complexes containing trithiocarbonate 1, 3, 4-thiadiazole moiety // Journal of King Saud University – Science 25,2013. – 157 p.
8. Kadirova Sh. A., Ishankhodzhaeva M. M., Parpiev N. A., Tozhiboev A., Tashkhodzhaev B., and Karimov Z. Tetragonal-Pyramidal Complex of Copper Nitrate with 2-Amino-5-ethyl-1, 3, 4-thiadiazole// Russian Journal of General Chemistry. – Vol. 78. – No. 12.2008. – 2398 p.
9. Toshmurodov T. T., Makhmudov U. S., Ziyaev A. A., Elmuradov B. Zh. Synthesis and crystal structures of 2-alkyltio-5-acetamido-1, 3, 4-tiadiazoles // Uzbek Biological Journal. – No. 4.2016. – 29 p.
10. Torambetov B. S., Kadirova Sh. A., Toshmurodov T. T., Ziyaev A. A. Quantum-chemical calculation of the 5-acetylamino-1, 3, 4-thiadiazole-2-ethylthione molecule and infrared spectroscopic study of its complex with zinc nitrate // International conference «Modern innovation: chemistry and chemical technology of acetylene compounds. Petroleum chemistry. Catalysis». – Tashkent. 2018. – 303 p.

Contents